Deliverable 6.5
Densification techniques test report

31st July 2024 Version Final

Dissemination level: Public

Lucy Mottram
Russell Hand

The University of Sheffield (USFD)
Department of Materials Science & Engineering
Sir Robert Hadfield Building
Mappin Street
Sheffield
S1 3JD

r.hand@sheffield.ac.uk
l.mottram@sheffield.ac.uk

This project has received funding from the Euratom research and training programme 2019-2020 under grant agreement No 945098.

Project acronym PREDIS	Project title PRE-DISposal management of radioactive waste	Grant agreement No. 945098

Deliverable No. D6.5	Deliverable title Densification techniques test report	Version Final
Type Report	Dissemination level Public	Due date M47
Lead beneficiary University of Sheffield (USFD)		WP No. 6

Main authors Lucy Mottram and Russell Hand (USFD)	Reviewed by Thierry Mennecart (SCK CEN) WP6 Leader	Accepted by Maria Oksa (VTT) Coordinator

Contributing authors Ewan Maddrell (NNL), Hélène Nonnet (CEA), Sam Walling (USFD), Claire Corkhill (USFD)	Pages 48

Abstract

Densification has primarily focussed on the use of hot isostatic pressing supported by some related cold-press and sinter work. These processes have been applied to several potential wastes primarily ion exchange resins, wet oxidation (wetox) wastes from Fenton oxidation and IRIS ashes.

Attempts to HIP polymeric ion exchange resins were unsuccessful as the polymeric wastes started to break down during the process to weld on the can lid, meaning that the HIP canisters could not be sealed.

HIPping of the simulant wetox wastes produced a series of solid multi-phase ceramic wasteforms. The phase assemblage of the wasteforms can be driven towards spinel by the increasing the fraction of Fe_2O_3 in the batch, and it may be possible to achieve a single phase spinel by optimising the HIPing conditions. There is some interaction between the HIP canister and the bulk material, to the detriment of the HIP canister wall, however not enough to warrant concern.

HIPping of the as-received IRIS ashes formed a solidified product which, at least partially, melted to form a crystalline multi-phase wasteform. Grinding of the ashes and additions of sodium aluminate or sodium tetraborate led to improved products with sodium tetraborate being the most successful additive, resulting in a glass-ceramic material in which the ash was almost completely melted.

An alternative approach involved additions of sodium silicate followed by cold pressing or granulation, followed by thermal treatment. This successfully produced denser products.

Keywords

Densification, Hot Isostatic Pressing (HIPping), wet oxidation waste, IRIS ashes

Coordinator contact

Maria Oksa
VTT Technical Research Centre of Finland Ltd
Kivimiehentie 3, Espoo / P.O. Box 1000, 02044 VTT, Finland
E-mail: maria.oksa.@vtt.fi
Tel: +358 50 5365 844

Notification

The use of the name of any authors or organization in advertising or publication in part of this report is only permissible with written authorisation from the VTT Technical Research Centre of Finland Ltd.

Acknowledgement

This project has received funding from the Euratom research and training programme 2019-2020 under grant agreement No 945098.

TABLE OF CONTENTS

1 Introduction

Densification has primarily focussed on the use of hot isostatic pressing supported by some cold-press and sinter work. The basics of the densification processes are outlined in Section 2. The densification of wastes from different parts of the PREDIS programme using these techniques has been investigated and the outcomes of these investigations are detailed in Sections 3, 4 and 5.

2 Densification equipment

2.1 Hot Isostatic Pressing (USFD and NNL)

The nuclear research HIP (AIP6-30H) at the University of Sheffield was commissioned in 2011 with maximum operating temperatures of 1350 °C (molybdenum furnace) and 2100 °C (graphite furnace) with a maximum pressure of 200 MPa (30,000 psi). The nuclear research HIP (AIP16-15HYK) at the National Nuclear Laboratory was commissioned in 2007, operating with a typical maximum temperature of 1320°C and a pressure of 100 MPa (14,500 psi). HIP samples are often prepared using straight-walled stainless steel (304) HIP canisters, though other engineered canisters which collapse in a pre-determined fashion, including controlled radial collapse cans and other HIP canister materials (Ni and Cu) are also utilised.

Wasteform production using a HIP typically involves the conversion of a powdered or granular material into a solid block. This is achieved by packing the loose material into a steel canister, which is sealed and then transferred to the HIP pressure vessel where both heat and pressure are applied. This results in a solid product fully encased within the steel container.

At USFD, material (ash, sludge, resin) is packed into the canister by filling partway with material, then pressing this into the canister with a short metal plunger (slightly smaller than the internal canister diameter) and applying 2 tons of pressure from a hydraulic press. This process is repeated until the canister is ~4/5 full. The lid is then screwed on, being careful to avoid any powder ingress into the threads (to ensure a clean welding process).

The canister lid is then welded into position prior to the bakeout process, where a vacuum is applied to the evacuation tube (atop the canister lid) inside a furnace at a specified temperature. This drives off any residual water and ensures that a vacuum is kept. After a set period (e.g. 12 h), the evacuation tube is crimped off and welded shut, resulting in a hermetically sealed canister.

Once the canister is prepared, it is placed within a secondary container (e.g. steel crucible) and loaded into the Hot Isostatic Press pressure vessel, which is then closed and prepared for operation.

Details of the canister sealing and bake out processes used in the NNL trials are given in Section 3.2.4.

The HIP process itself involves the application of both heat (applied *via* a furnace within the HIP) and pressure (applied isostatically *via* argon gas). Typically, both temperature and pressure are both increased concurrently until the desired temperature and pressure are achieved. The canisters are held at these conditions for a given period of time (typically 2-4 h), before both temperature and pressure are lowered in a controlled manner. This results in uniform application of pressure across the canister while at temperature, with sample densification, and a reduction in the HIP canister volume (Figure 2-1).

Figure 2-1. HIP canister with evacuation tub attached, before (left) and after (right) HIP processing.

Following HIPing, the canisters are sectioned and opened using a Buehler IsoMet 1000 Precision Cutter equipped with a cubic boron nitride wafering blade. Both the top and bottom sections of the are canisters removed, followed by the two opposing sides (Figure 2-2). This allows the manual removal of the remaining two canister sides (when the wasteform does not bind to the steel), resulting in a solid monolith and several offcuts for further analysis.

Solid off-cut pieces removed from the canisters are utilised for XRD analysis. The bottom of the canister is used for SEM analysis (allowing analysis of both bulk, and wasteform-canister interface), embedding the entire bottom piece within cold setting epoxy resin, then sequentially grinding and polishing to a 1 µm finish. The resulting SEM stub is depicted in Figure 2-3.

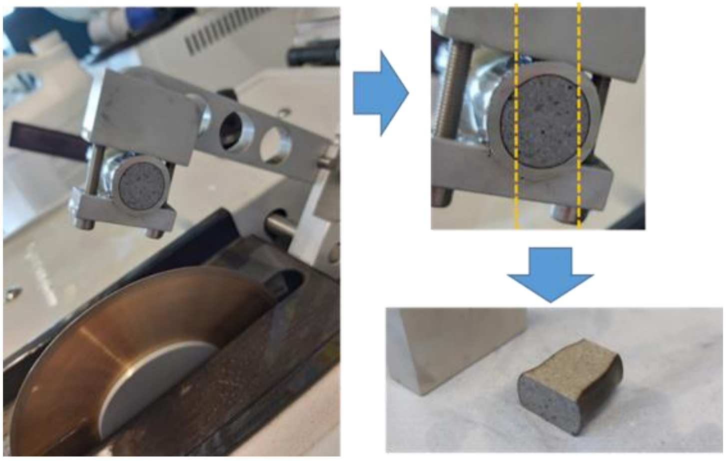

Figure 2-2. Sectioning of canister post-HIP.

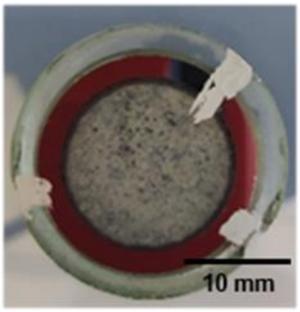

Figure 2-3. Sample prepared for SEM analysis, after embedding in resin, grinding/polishing, then carbon coating and applying conductive silver dag.

2.2 Hot Pressing (KIPT)

Hot pressing utilises uniaxial pressure during heating to achieve a denser product; powders are packed into a die and then the required pressure is applied throughout thermal treatment, pressures and temperatures applied by KIPT are specified in Section 5.2.1.

2.3 Cold Pressing/Compaction followed by thermal treatment (USFD and CEA)

Cold pressing and sintering (CPS), referred to as compaction by CEA, utilises uniaxial pressure prior to thermal treatment. Powders are packed into a die and subjected to pressure in a uniaxial press, after which samples undergo thermal treatment, where possible details of the pressure and temperature used are given in each relevant section.

2.4 Granulation followed by thermal treatment (CEA)

The forming of granulates prior to thermal treatment as a densification method was undertaken by CEA and is described in Section 4.2.

3 Ionic Exchange resins

3.1 Direct Disposal + HIP (USFD)

The potential for treatment of polymeric material via HIP was investigated. The polymeric material chosen was a mixed bed cation-anion nuclear grade exchange resin (Amberlite IRN-150, Figure 3-1). This is the same resin that was treated *via* Fenton wet oxidation within WP 6.3.

The treatment of polymeric materials *via* HIP presents challenges due to mismatch between the high temperatures preferred for wasteform consolidation (especially within steel canisters, which typically only begin to soften at temperatures of >500 °C), and the low temperatures required to avoid thermal degradation of the polymeric material. The minimum temperature for a HIP run is likely to be ~100-130 °C based on the temperature rise caused by compression of argon into the HIP pressure vessel.

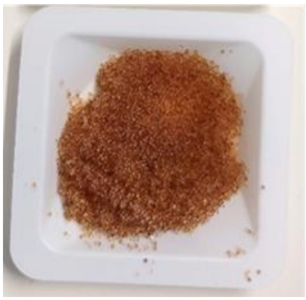

Figure 3-1. Photograph of IRN-150 resin.

Two trials to investigate the feasibility of HIP to immobilise ion exchange resin were undertaken. The first focused on direct immobilisation (*i.e.*, no additive), while the second explored the potential for embedding the resin within a separate polymer matrix of low density polyethylene (LDPE; Thermo Scientific, powder, low density, 500 µm). As the aim was not to decompose the material, rather to consolidate or potentially melt the resin, the maximum processing temperature was key. Literature suggested the resin undergoes decomposition from ~300 °C onwards, whilst LDPE decomposition requires higher temperatures, ~390 °C (though melting occurs before this temperature) [5-7].

The resin was prepared by drying overnight in an oven at 90 °C to remove as much water as possible. Two trials were planned:

1. Dried IRN-150
2. Dried IRN-150 + LDPE

HIP qualification / bakeout was scheduled to be performed at room temperature under vacuum, then intended to be HIPed at 200 °C under 100 MPa pressure. It was unknown whether the HIP canister would deform well at this temperature. Typically using HIPing, the combination of temperature (enough to begin softening the steel, >500 °C) and pressure allows the canisters to be compressed down and around the waste whilst protecting / minimising stress on the welds. Using such low temperatures, with small canisters that have relatively thick steel walls, may not produce ideal deformation. Despite this, the constraint on the upper temperature was the polymer degradation temperature.

3.1.1 Dried IRN-150 direct HIP

Dried IRN-150 resin was packed directly into a stainless steel HIP canister using a uniaxial press and metal plunger (as per the IRIS ash sample packing). The resin flowed into the canister smoothly, although it did not pack densely even with the application of 2 tons of pressure (some resin beads were heard to audibly crack). A total of 2.85 g of dried resin was packed into the canister, as demonstrated in Figure 3-2, which shows the canister before the lid was screwed on.

Figure 3-2. Trial 1 after packing (before addition of lid).

During the welding of the canister, which is a high temperature process, a dark brown pungent liquid oozed out of an as-yet unwelded section of the canister lid; this gap in the weld is shown in Figure 3-3. The technician attempted to clean the top of the canister with a wire brush, and resume welding; however, the liquid began oozing out again preventing completion of the weld. It was concluded that this liquid was likely to be melted resin that formed during the high temperature welding process. Due to the potential degradation of the resin within, and inability to seal, the HIP canister, this sample was not taken forward for HIP treatment.

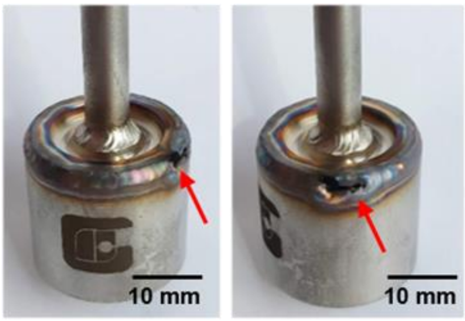

Figure 3-3. Trial 1 after welding, showing incomplete weld.

3.1.2 Dried IRN-150 + LDPE

A canister was packed using dried IRN-150 and LDPE powder. 10 g of dried IRN-150 was mixed with 10 g LDPE and mixed together manually for 5 minutes (resulting in a 50% dried resin loading). A total of 3.6 g of this combined material was packed into a HIP canister using a uniaxial press and a metal rod. This canister packed very well, with notable compaction due to the fine LDPE powder that helped to keep the resin in place during packing. Figure 3-4 shows a photograph of the packed resin / LDPE batch in the canister prior to screwing on the lid.

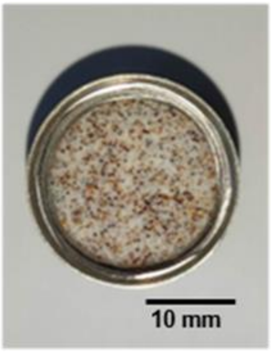

Figure 3-4. Trial 2 after packing (before addition of lid).

Although this canister packed well, a similar melting event occurred during the attempt to weld the lid. Although the technician attempted to complete the weld quickly (and at a lower power setting than the previous failed attempt), liquid material escaped from the canister during welding, leaving an unwelded section (photographed after cooling in Figure 3-5).

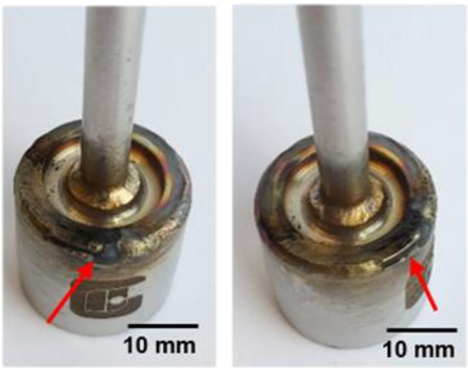

Figure 3-5. Trial 2 after welding, showing incomplete weld.

Given that the material inside the canister was degraded by the temperatures induced by welding, and since the HIP canister could not be sealed, this sample was also unable to be HIPped. A potential solution might be to use larger, taller canisters, with 50% packing, where the top of the canister could be filled with steel spacers to mitigate the degradation of the polymer. However, there would still be a high risk that the polymer within the canister had been exposed to high enough temperatures to cause polymer melting or thermal degradation.

Using the equipment and canisters available at USFD, it was deemed that HIPping of polymeric material is not achievable and no further attempts were made to HIP polymeric materials within the PREDIS project.

3.2 Wet oxidation (Wetox) + HIP (USFD + NNL)

3.2.1 Wet oxidation (wetox) waste

This section of the work package (WP 6.5) relates to Hot Isostatic Pressing (HIP) of simulant residues arising from Fenton wet oxidation (wetox) of organic ion exchange resins, performed within the scope of WP 6.3. The Fenton process utilised involves the addition of hydrogen peroxide and a mixed iron/copper sulfate catalyst, combined with heat (<100 °C) and agitation to degrade the organic material. This results in a sodium sulfate rich liquid waste, with an iron and copper rich sludge. Processing of nuclear ion exchange resins (e.g. from primary circuit decontamination) through this process will result in the partitioning of many radionuclides into the iron and copper-rich sludge. It is proposed that the HIP process may be applied to filtered and dried sludge.

WP 6.3 specifically treated a mixed bed nuclear grade cation:anion exchange resin (IRN-150). Characterisation of the resulting sludge revealed a poorly crystalline copper and iron rich material (roughly equimolar Fe:Cu), which upon heating to 600 °C (HIP canister bakeout temperature) produced a mixture of Fe_2O_3 and CuO. This mixture was used as a simulant material (required due to the high volume reduction achieved during the wet oxidation process), which would allow aligning between USFD and NNL scaled up HIP canisters. The wet oxidation rig at USFD produces very minor quantities of sludge per run, making this unfeasible to produce enough material for a full HIP campaign.

Preliminary investigations into the potential for HIP processing of this material involved cold pressing and sintering pellets of varying compositions, to determine their stability at varying temperatures and the resulting phase assemblage. These studies were designed to help formulate compositions for the small-scale HIP trials.

3.2.2 Wet oxidation (wetox) + CPS scoping trial (USFD)

This preliminary trial investigated three different formulations along the CuO-Fe_2O_3 binary phase diagram, starting from the CuO/(CuO+Fe_2O_3) value determined from the real wet oxidation sludge (0.67 – an equimolar Cu:Fe composition). The original intention of this work was to constrain the milling parameters and chemical precursors prior to developing a HIPped wasteform at a small scale. Literature data [4] indicated that this composition should result in the formation of delafossite ($CuFeO_2$), which was targeted in the first formulation. The addition of extra Fe_2O_3 should then push the system towards the formation of spinel ($CuFe_2O_4$): the second formulation. The formation of a spinel phase (formulation number three) would be beneficial for retention of certain radionuclides (e.g. activation products) likely to be within real wet oxidation sludge, such as Ni, Co and Mn. These could potentially form $NiFe_2O_4$, $CoFe_2O_4$, and $MnFe_2O_4$, respectively, with an excess of Fe_2O_3.

Literature also suggested that the maximum processing temperature would be ~1080 °C before melting occurs for much of the $CuO\text{-}Fe_2O_3$ phase diagram (Figure 3-6).

On this basis, three formulations were part of the preliminary trial, starting from the wet oxidation sludge composition, then working towards the Fe_2O_3 end of the phase diagram, with the aim to forming spinel in the third composition (all as molar formulations), as follows:

- **(1)** 1 CuO : 0.5 Fe_2O_3 ($CuO/(CuO+Fe_2O_3) = 0.67$) → target delafossite ($CuFeO_2$))
- **(2)** 1 CuO : 0.67 Fe_2O_3 ($CuO/(CuO+Fe_2O_3) = 0.60$) → target delafossite + spinel (e.g. $CuFe_2O_4$)
- **(3)** 1 CuO : 1.22 Fe_2O_3 ($CuO/CuO+Fe_2O_3) = 0.45$) → target spinel

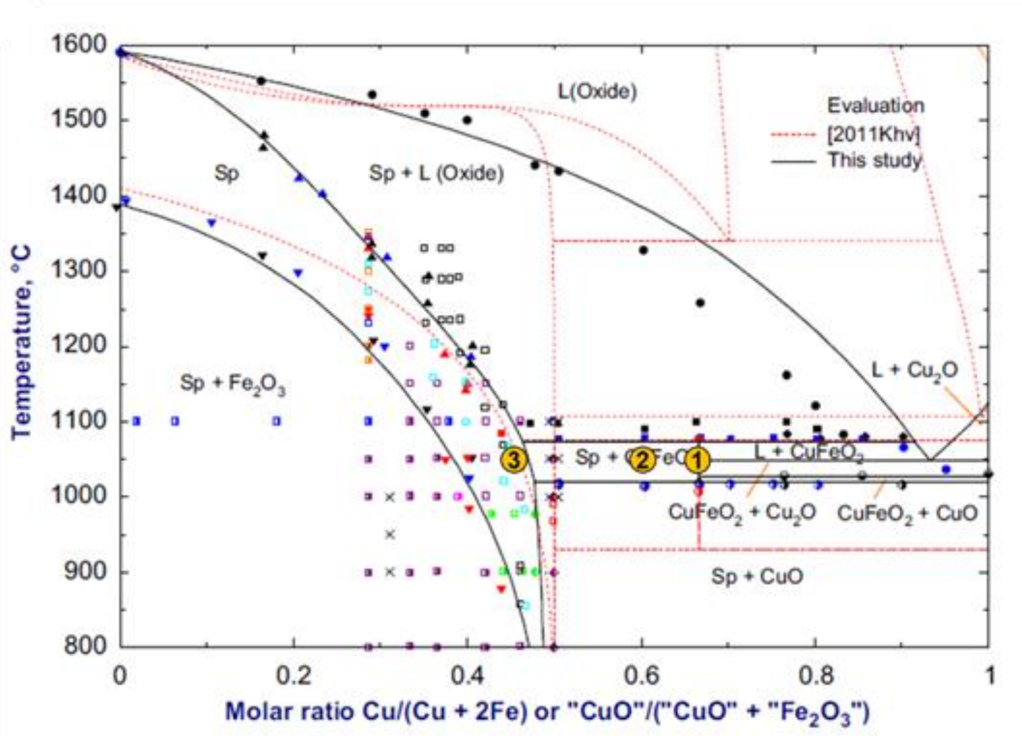

Figure 3-6. $CuO\text{-}Fe_2O_3$ phase diagram with target formulations labelled, adapted from Shishin, et al. [4].

For each formulation, the required quantities of Fe_2O_3 (98%, Alfa Aesar) and CuO (99%, Alfa Aesar) were weighed out, then intimately mixed by ball milling in isopropanol for 10 minutes (at 500 rpm using ZrO_2 mill pot and 3 mm milling media). The resulting slurry was recovered from the milling media, then dried in an oven at 90 °C. Two pellets were pressed for each formulation, using 0.5 g of material per 10 mm diameter pellet. All pellets were placed on a zirconia boat (Figure 3-7), and heated up to 1050 °C in a muffle furnace (10 °C/min ramp rate, standard atmospheric conditions) and held at temperature for 4 hours.

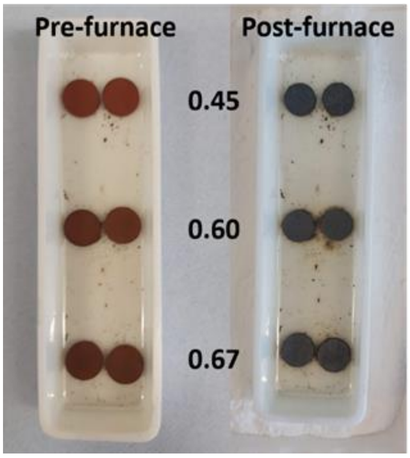

Figure 3-7. Pellets pre- and post-furnace, arranged by CuO/(CuO+Fe_2O_3) ratios.

All formulations appeared to sinter well with no noticeable melting, although both the CuO/(CuO+Fe_2O_3) = 0.60 and 0.67 formulations did stick to the crucible, which possibly suggests that a small amount of liquid phase was formed.

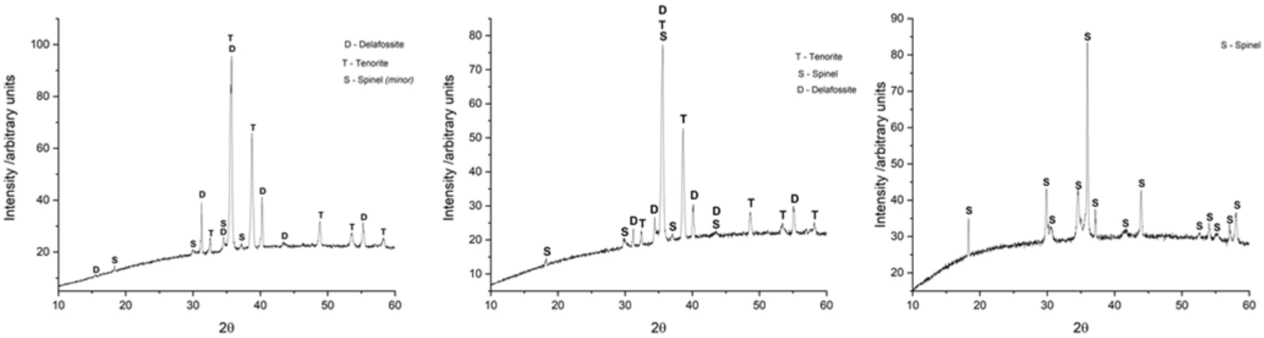

Figure 3-8. XRD pattern collected from sintered formulations a) CuO/(CuO+Fe_2O_3) = x = 0.67, b) x = 0.60 and c) x = 0.45.

XRD patterns collected from the pellets (Figure 3-8) revealed that all formulations produced a crystalline product, with both the 0.60 and 0.67 formulations forming multiphase ceramics, with reflections assigned to delafossite, spinel and tenorite (CuO). An increase in Fe was found to result in an increase in the relative amount of spinel present, with the highest Fe concentration formulation ((CuO/CuO+Fe_2O_3) = 0.45), presenting an XRD pattern with reflections which were all attributed to a spinel phase, suggesting that a single phase spinel had been produced.

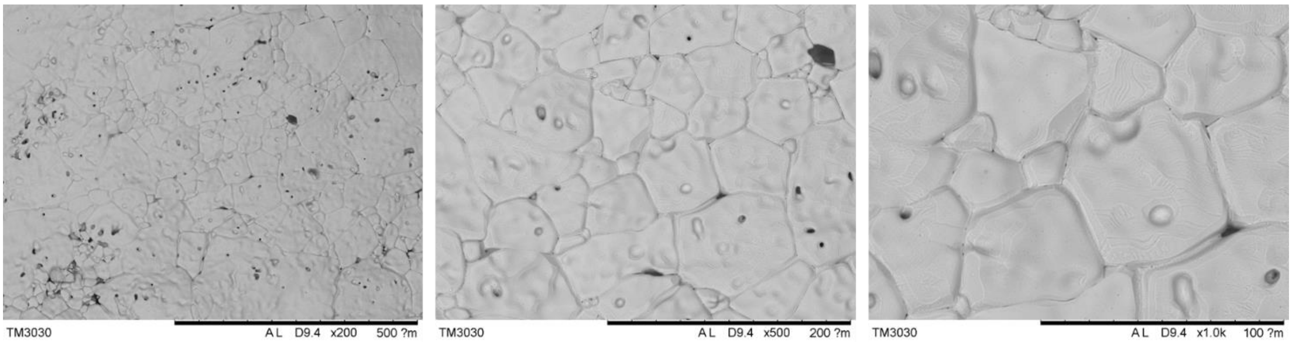

Figure 3-9. SEM images collected from formulation CuO/(CuO+Fe_2O_3) = 0.45.

The 0.45 formulation pellet was broken to enable the collection of SEM data along a fracture surface. SEM images (*Figure 3-9*) showed that the sample had sintered well, with low porosity. EDX element maps (

Figure 3-10) confirmed that this formulation had produced a single phase. Analysis of EDX data provided an estimated composition of $Fe_{2.11(5)}Cu_{0.89(3)}O_4$.

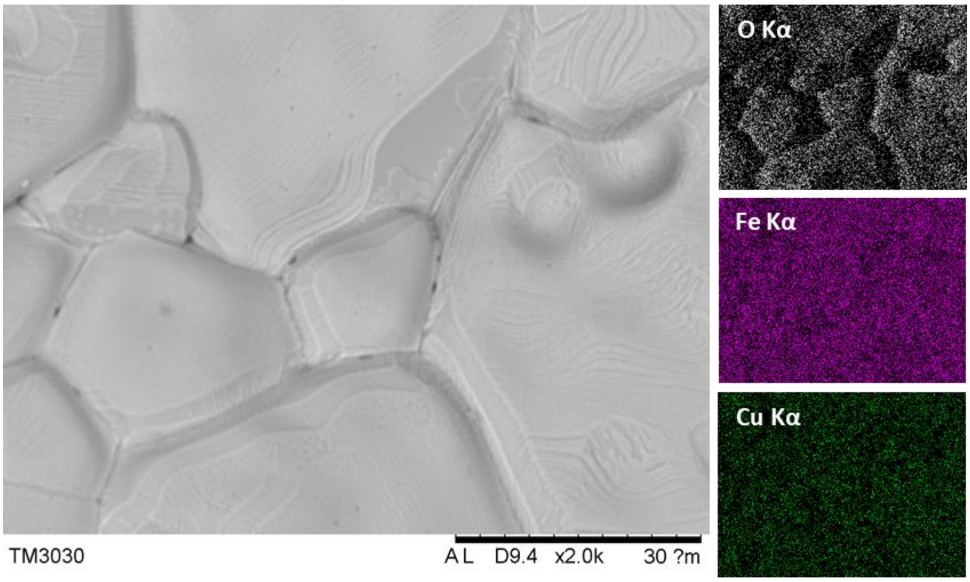

Figure 3-10. SEM image and EDX data collected from formulation CuO/(CuO+Fe_2O_3) = 0.45.

3.2.3 Wet oxidation (wetox) waste + HIP (USFD)

The same three formulations were then prepared for HIPping. Powder was packed into steel, straight sided HIP canisters (Figure 3-11) and the canisters were baked out at 300 °C for at least 12 h to ensure material was dry before sealing shut the canisters. The HIP canisters were all processed with a 10 °C/min ramp up to a maximum temperature of 1250 °C, with a 2 h dwell at the maximum temperature at a 100 MPa pressure. These conditions were undertaken as they are set of standardised thermal treatment conditions which have been applied to other materials HIPped at the USFD, including the IRIS ashes (see Section 4.3), to enable direct comparison. The canisters were all successfully baked out, sealed and HIPped. Then canisters were then cut open and sectioned to enable characterisation by SEM and XRD.

Figure 3-11. Photographs of HIP canisters before and after HIPing.

XRD data from bulk material removed from HIP canisters are shown in Figure 3-12. All of the formulations produced crystalline, multiphase ceramic materials. The reflections in the XRD patterns were attributed to three phases with the structures of tenorite, delafossite and spinel, with the nominal compositions of CuO, $FeCuO_2$ and Fe_2CuO_4 respectively. As noted in Section 3.2.2 these phases were also identified in the sintered pellet samples. In line with the sintered samples there is a clear increase in the relative fraction of spinel in the $(CuO/CuO+Fe_2O_3) = 0.45$ formulation compared to the $(CuO/CuO+Fe_2O_3) = 0.60$ and $(CuO/CuO+Fe_2O_3) = 0.67$ formulations. However, whereas the sintered pellet produced with the $(CuO/CuO+Fe_2O_3) = 0.45$ formulation was a single phase spinel, the $(CuO/CuO+Fe_2O_3) = 0.45$ formulation HIPped sample is not a single phase ceramic. One likely cause of this is the higher temperature used during HIPping (1250 °C), which is above the ideal temperature range to achieve a single phase spinel identified from the Fe_2O_3:CuO phase diagram (see Figure 3-6). The XRD pattern for the $(CuO/CuO+Fe_2O_3) = 0.60$ formulation displayed a preferred orientation for the tenorite $(20\bar{2})$ reflection; this may be due to the measurement conditions as XRD data were collected from sectioned monoliths, not powders.

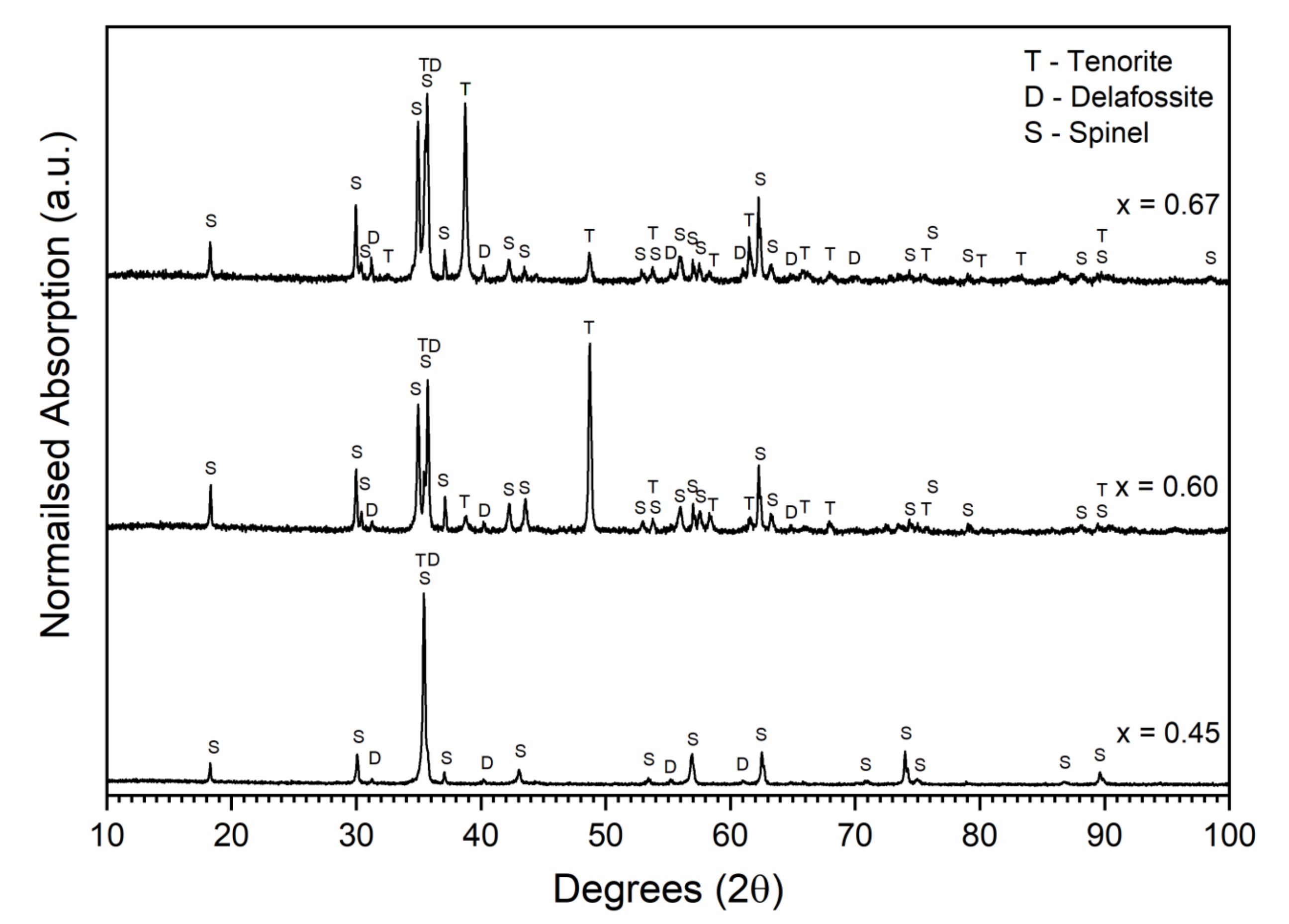

Figure 3-12. XRD patterns from HIPped formulations: $CuO/(CuO+Fe_2O_3) = x = 0.67, 0.60$ and 0.45.

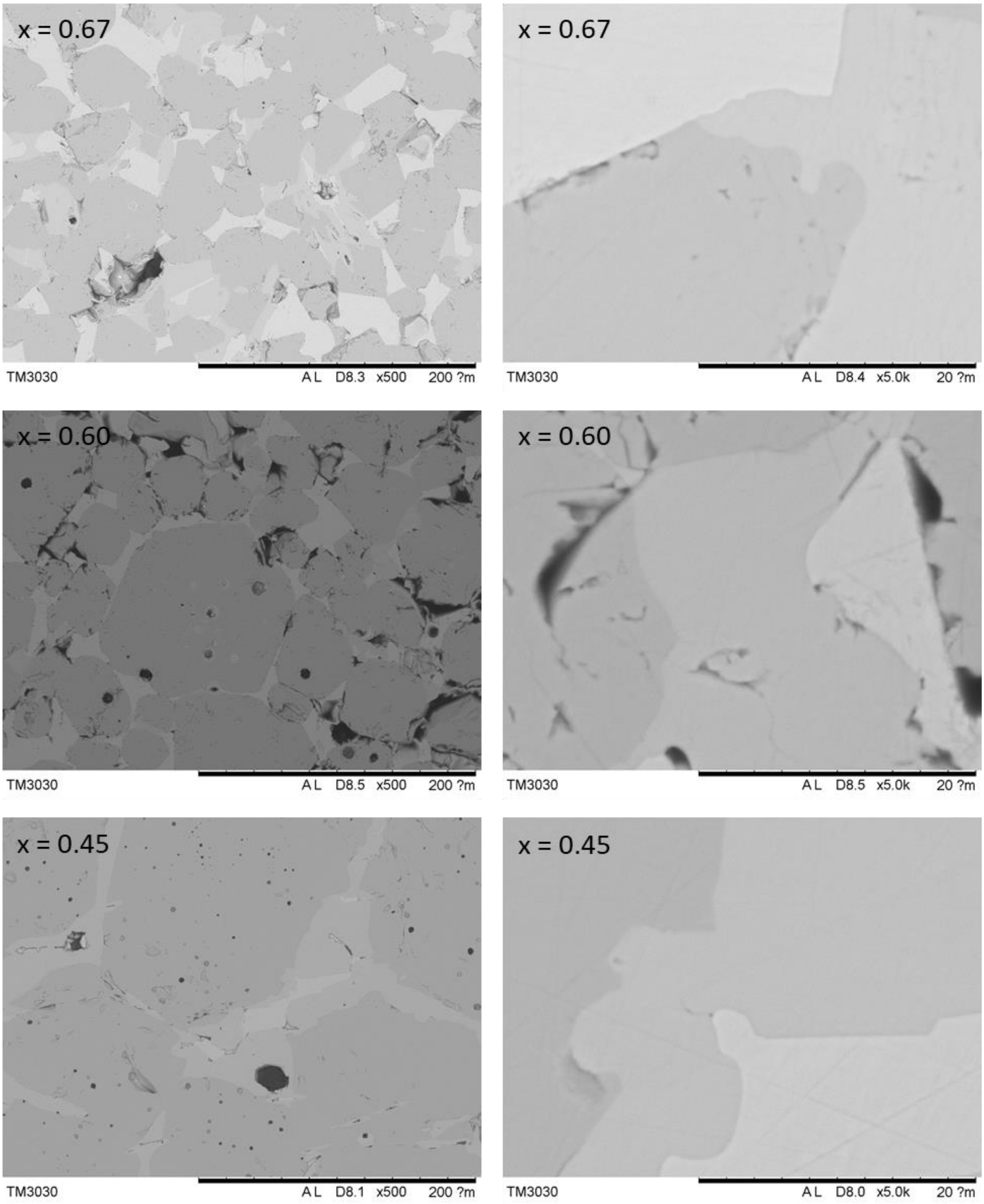

Figure 3-13. SEM micrographs of cross sections of HIPped formulations $CuO/(CuO+Fe_2O_3)$ = x = 0.67, 0.60 and 0.45.

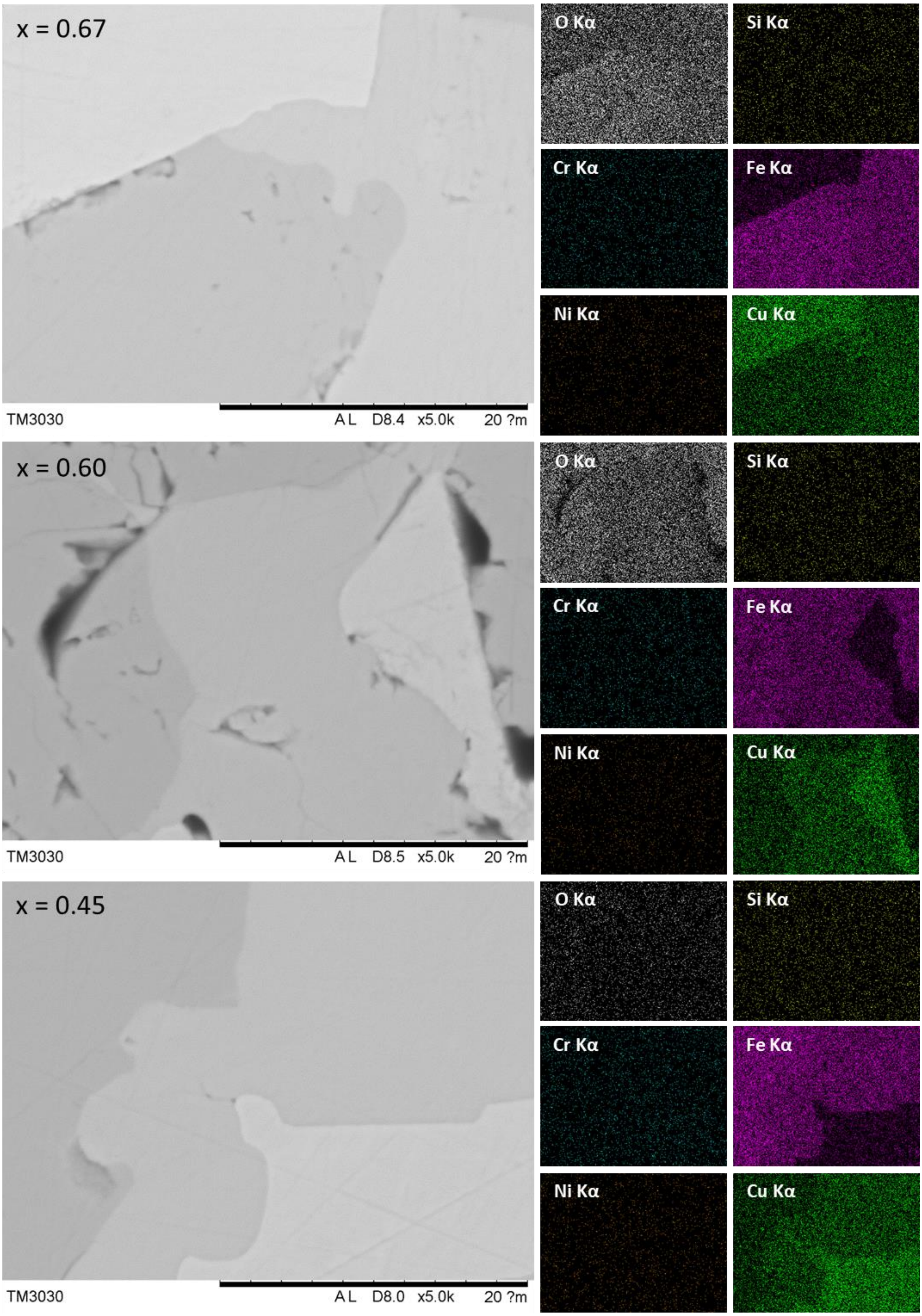

Figure 3-14. SEM micrograph and EDX maps of bulk region of formulations $CuO/(CuO+Fe_2O_3)$ = x = 0.67, 0.60 and 0.45.

SEM micrographs collected from the bulk region of the three HIPped formulations are shown together in Figure 3-13, to enable comparison of microstructure and phase assembly. The SEM data from all three formulations confirmed the presence of three phases in each sample. The lightest phase contains the most of the heaviest element present, Cu and therefore the darkest phase the least Cu and most Fe; this was confirmed by EDX mapping (Figure 3-14). The compositions of the three different phases, were confirmed by EDX (Table 3-1) to be a) darkest: spinel, b) medium: delafossite and c) lightest: tenorite.

Table 3-1. Estimates of phase compositions from EDX analysis, with nominal compositions of tenorite, delafossite and spinel given for comparison.

	Phase Composition (Molar ratio)								
	Tenorite [CuO]			**Delafossite [$FeCuO_2$]**			**Spinel [Fe_2CuO_4]**		
Formulation	**Fe**	**Cu**	**O**	**Fe**	**Cu**	**O**	**Fe**	**Cu**	**O**
0.67	0.11(1)	0.89(2)	1.00	1.00(2)	1.00(3)	2.00	2.03(4)	0.97(3)	4.00
0.60	0.14(1)	0.86(2)	1.00	1.06(2)	0.94(3)	2.00	2.11(4)	0.89(2)	4.00
0.45	0.13(1)	0.87(3)	1.00	1.09(3)	0.91(3)	2.00	2.14(5)	0.86(3)	4.00
Nominal Composition	0.00	1.00	1.00	1.00	1.00	2.00	2.00	1.00	4.00

SEM micrographs from the bulk of the $CuO/(CuO+Fe_2O_3) = 0.67$ formulation (Figure 3-13) show that the major phase present is spinel, with regions of tenorite and smaller areas of delafossite between the grains of spinel. There is also some porosity present, but less than was observed in the sintered pellet (Figure 3-9).

SEM micrographs collected from the $CuO/(CuO+Fe_2O_3) = 0.60$ and 0.45 formulations show a trend of both an increase in the fraction of spinel present, and the size of the spinel grains. The micrographs of the $CuO/(CuO+Fe_2O_3) = 0.60$ formulation reveals larger grains of spinel with some regions of tenorite and delafossite, in the $CuO/(CuO+Fe_2O_3) = 0.45$ formulation the grains of spinel are even larger and tenorite and delafossite only occur at some of the grain boundaries between spinel grains. In the $CuO/(CuO+Fe_2O_3) = 0.45$ formulation, delafossite rather than tenorite appears to be the dominant secondary phase, which is in agreement with the relative intensity of peaks assigned to delafossite and tenorite in the XRD pattern of the $CuO/(CuO+Fe_2O_3) = 0.45$ formulation (Figure 3-12). All formulations contained some porosity, which would reduce the wasteform’s resistance to dissolution, but such porosity may be reduced by an optimisation of the HIP processing conditions.

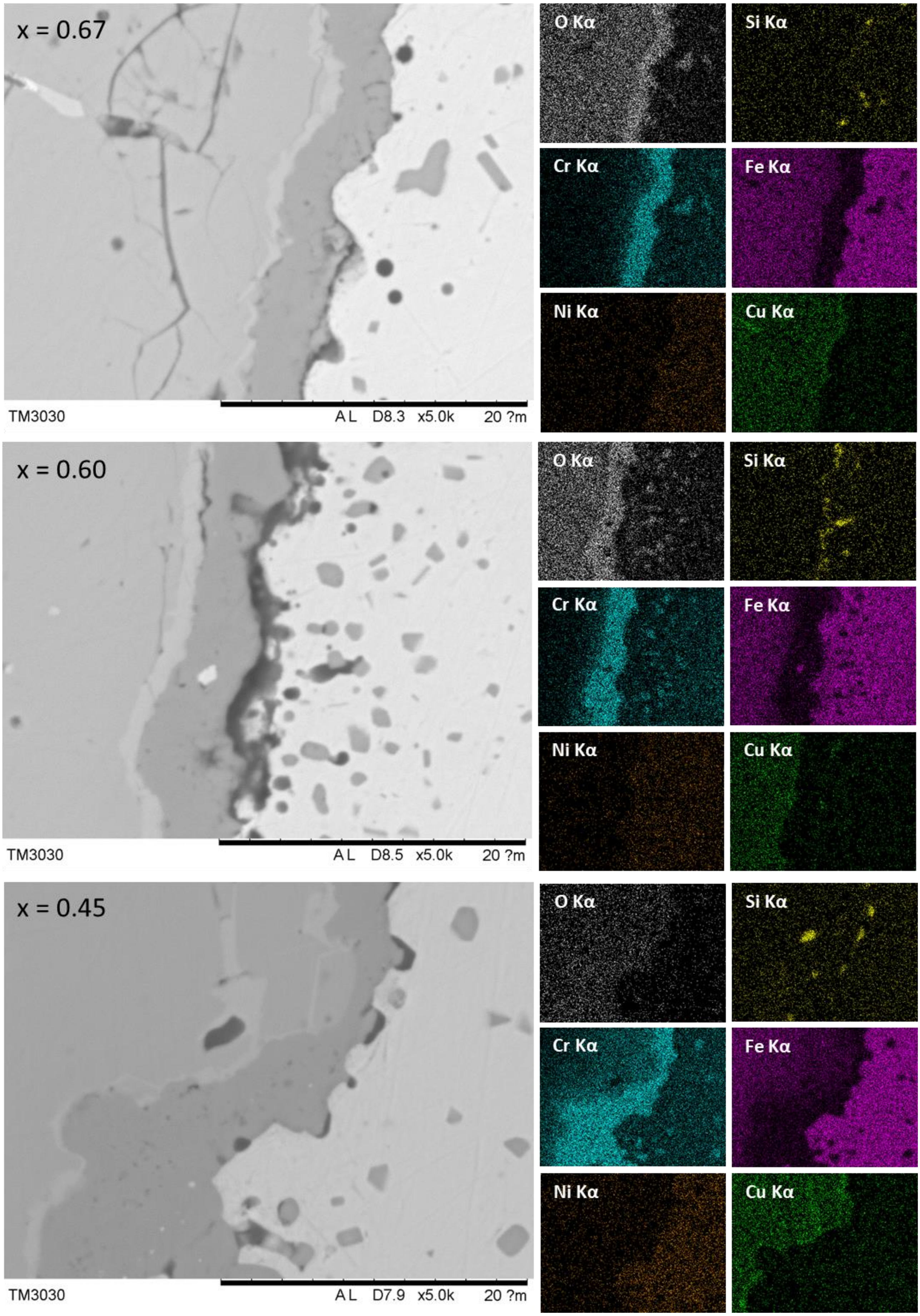

Figure 3-15. SEM micrograph and EDX maps of material-HIP canister interactions of formulations CuO/(CuO+Fe_2O_3) = x = 0.67, 0.60 and 0.45.

Figure 3-15 shows SEM micrographs and EDX element maps collected from the region where the HIP canister wall is in contact with the HIPped material for each formulation. All formulations interacted with the HIP canister wall, with two intermediate phases formed between the canister and the bulk material. The migration of Cr from the stainless steel canister to the bulk wasteform to form a darker phase can be observed in all three formulations, as can the formation of a brighter phase which may be rich in Cu. In some samples the bulk material appeared to have shrunk during cooling, with cracks and gaps observed between the wasteform and the bulk material. Some erosion of the HIP canister wall may have occurred, which can be a concern as significant erosion of the HIP can wall can reduce the structural integrity and performance of the HIP canister, however the erosion which occurred here is minimal, and not a cause for concern.

In summary, HIPping of the simulant wetox wastes has produced a series solid multi-phase ceramic wasteform. The phase assemblage of the wasteform can be driven towards spinel by the increasing the fraction of Fe_2O_3 in the batch, and it may be possible to achieve a single phase spinel by optimising the HIPping conditions. There is some interaction between the HIP canister and the bulk material, to the detriment of the HIP canister wall, however not enough to warrant concern.

3.2.4 Wet oxidation (wetox) waste + HIP (NNL)

NNL were tasked with producing scaled up HIP products from the wet oxidation simulant at USFD, to demonstrate the technical ability to upscale this process. The original intention was that these trials would be informed by data arising from the trials at USFD, however due to delays in the USFD HIP trials, consequent on the USFD being down for an extended period following a serious near miss, the NNL trials had to be undertaken before the USFD trials were completed.

The scale of the HIP can was a four convolution controlled radial collapse design with an internal volume of 7.9 litres (approximately 30 cm high by 20 cm diameter). It was realised that the ion exchange resin treatment method under development was not going to be able to produce the required quantity of feed material. The decision was made to use standard laboratory oxide feeds, and for simplicity to limit these to Fe_2O_3 (Fisher product 012375) and CuO (Fisher product 012299). Two blend ratios were identified:

1. 1 CuO : 2.44 $FeO_{1.5}$ i.e. $(CuO/CuO+Fe_2O_3) = 0.45$
2. 1 CuO : 1 $FeO_{1.5}$ i.e. $(CuO/CuO+Fe_2O_3) = 0.67$

These molar ratios translated approximately into 1 : 2.5 and 1 : 1 based on mass.

Because of the required quantities of the powder blends required to fill the HIP cans it was decided to blend batches in a 2 litre high density polyethylene (HDPE) jar. To improve mixing 13 mm alumina milling balls were used with water as a carrier liquid to prevent the cohesive powders agglomerating. The target was a paint-like consistency for the slurry. The blending process was conducted with a Turbula T2F mixer.

3.2.5 HIP Can One

This HIP can was targeting blend ratio 1. Each batch composition was nominally 400 g CuO and 1000 g Fe_2O_3 with 550 g H_2O and 1000 g of milling balls. The mixing time and Turbula speed setting do not appear to have been recorded. Two batches were prepared per day with the slurries being dried overnight at 110 ºC. Twelve batches were produced. After drying the batches were stored collectively in a larger container.

For HIP can filling, 1400 g batches of the powder blend were placed in the HIP can and subjected to 1 minute on a vibratory table to improve packing. This was repeated until the HIP can was full. When the HIP can was full the lid was welded in position.

HIP can bakeout was conducted in a pottery kiln. The bakeout cycle was to heat the kiln to 600 ºC at 5 ºC per minute and then hold at 600 ºC for 4 hours. The HIP can was connected to a vacuum pump throughout the cycle. At the end of the hold period the evacuation tube on the HIP can was crimped. It was observed that the HIP can began to bloat, extending along its axis. The bloated can is shown alongside a non-deformed can in Figure 3-16. The increase in HIP can height is about 4.5 cm.

The cause of the bloating is not known for sure. A small amount of surplus feed material was subjected to an equivalent thermal cycle to the bakeout process in an open crucible. The proportionate mass loss was approximately double the mass loss measured for the HIP can. If the mass loss is attributed to adsorbed water that had not been removed during the drying process, this indicates that there was probably residual water still remaining in the HIP can. During bake out under vacuum water vapour was being removed. After the HIP can is sealed, the water vapour can no longer be removed and will start to pressurise the inside of the can, leading to bloating. As the HIP can cools the water vapour will condense, potentially leaving a partial vacuum inside the HIP can. Given the presumed presence of water in the HIP can, it was decided that it would be unwise to proceed with the HIP cycle.

Figure 3-16. Bloated HIP can one alongside a non-deformed HIP can of identical design.

3.2.6 HIP Can Two

This HIP can was targeting blend ratio 2. Each batch composition was nominally 900 g CuO and 900 g Fe_2O_3 with 500 g H_2O and 1000 g of milling balls. The blending and initial drying was the same as for HIP Can One. To increase water removal a subsequent drying stage, overnight at 240 ºC was used.

The HIP can was then cycled through the same bakeout profile three times without a vacuum being applied, and weighed when cold the next morning. After three cycles there was confidence that no further mass loss was being observed and a fourth bakeout cycle was conducted under vacuum and the HIP can was sealed.

The HIP cycle had a dwell at 1000 ºC and 100 MPa for 2 h. The temperature was specified to ensure that the eutectic in the CuO-Fe_2O_3 phase diagram was not exceeded. The HIP can after the HIP cycle is shown in Figure 3-17. The individual lobes have consolidated as intended, but the lobes have sprung apart as the HIP pressure was released. This is strongly indicative of gas within the HIP can.

Figure 3-17. HIP can two showing well consolidated lobes which have sprung apart as the HIP pressure was released.

The initial method for interrogating this HIP can was X-ray radiography. An image from this method is shown in Figure 3-18. This shows a clear fissure running between the two central lobes. Fissures also start at the outer two folds between lobes and then propagate into the outer lobes.

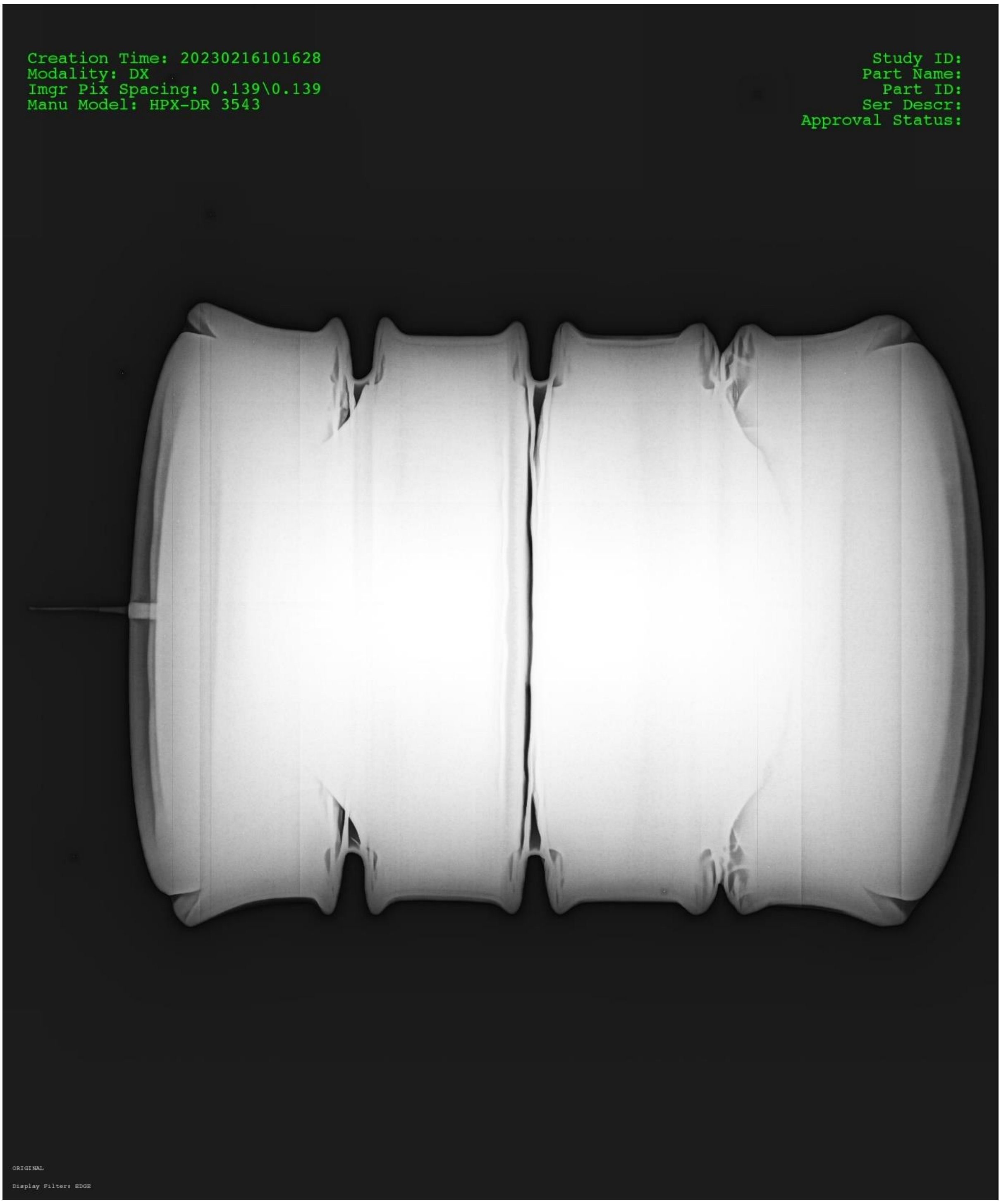

Figure 3-18. X-ray of HIP can two showing the fissures between lobes.

Further characterisation requiredd progressive destructive analysis and was undertaken by Lucideon (Staffordshire, UK). The first stage was to collect and analyse any gas within the HIP can. A 3.5 mm drill bit was used to drill into the fold between the two central lobes, and the gas liberated was then collected. The report from Lucideon states:

“On breaking through the outer layer of the can there was a strong release of gas which caused a fountain of water, confirming the presence of gas in the void space. The breakthrough point was entire and quicker than expected, and the release of gas was so strong that it was not possible to place the syringe fast enough to collect a large volume of the gas. As a result, only 80-100 ml of gas was collected. This may affect the results as explained below.

Table 3-2 Gas Volumes and Composition of Collected Gas from HIP Can produced by Lucideon

Gas	**Amounts**
Gas volume,	80 – 100 cm^3 at STP
CO_2	2.15 %
H_2	67 ppm
O_2	11.0 %
N_2	82.1 %
C_2H_6	Trace

“The results show that the gas collected was predominantly nitrogen with significant amounts of oxygen, carbon dioxide and traces of ethane and hydrogen.

“It is believed that only the oxygen, carbon dioxide, hydrogen and ethane are from within the HIP can. Tedlar bags are manufactured with nitrogen sealed within to stop the layers sticking together. In usual practice, the bags are filled and emptied to remove the residual nitrogen, which was not possible on this occasion because of the low volume of gas collected. Therefore, with a total volume of <100ml, the nitrogen content is likely to be from the residual nitrogen in the tedlar bag.

“The contents of the HIP can were identified as CuO and Fe_2O_3. The likelihood is that the copper oxide may be reducing to release some of the oxygen. The presence of carbon dioxide, hydrogen and ethane are not so easily explained but indicate the presence of a hydrocarbon, combustion products or pyrolysis products.”

The explanations behind the occurrence of some of the gases feel slightly speculative and are included here for completeness. An alternative explanation for the CO_2 might be that it results from wear debris picked up during the powder blending process. The O_2 could be explained by partial auto-reduction of CuO to Cu_2O. Although O_2 would be expected to react with the HIP can walls, if the ceramic near the HIP can walls has densified then the O_2 will not be able to react. The O_2 then pressurises the core of the HIP can leading to cracking when the HIP pressure is released. Again, this is speculative, and would require an evaluation thermodynamic data, or appropriate experimental work, to establish credibility.

The second stage of destructive analysis involved sectioning the HIP can to remove a “cake slice”. The HIP can after this sectioning process is shown in Figure 3-19. This shows the fissures explicitly, confirming the accuracy of the X-ray imaging.

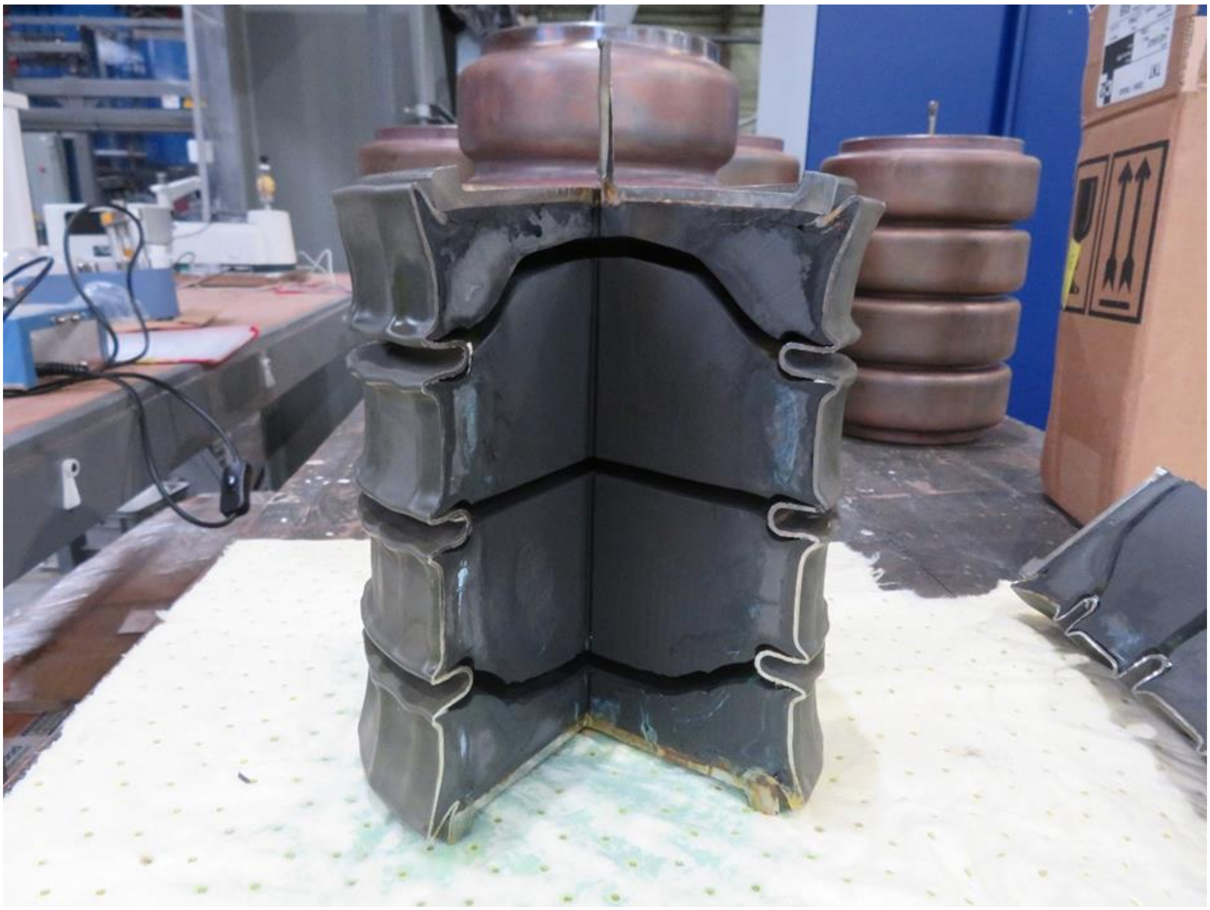

Figure 3-19. HIP can two after sectioning.

The results from the two HIP cans are disappointing. In particular, for HIP can two there is no clear explanation of what has happened within the HIP can to cause the fissures. One option for a third HIP can was to dry blend the CuO and Fe_2O_3, but this would have departed even further from being a valid simulant, so was not undertaken at this time.

Given the problems with the HIP runs and that a mixture of CuO and Fe_2O_3 is necessarily a simplified simulant of the wetox waste, a more appropriate forward direction might be to identify a method by which a more representative simulant can be prepared at the scale required. A simulant preparation method avoiding HDPE or other polymers would avoid one of the hypothesised causes of HIP can preparation. It would not remove any risk of CuO auto-reduction.

3.2.7 Comments on scale up (USFD)

Work undertaken by the USFD has shown that the simulant wetox wastes can be successfully HIPed at a smaller scale. However, NNL's attempts to HIP simulant wetox wastes were unsuccessful so proof of scale up has not yet been achieved. Comparison and discussion of approach has also highlighted potential barriers to scale up. To produce the smaller batches of simulant waste at USFD isopropanol was used as a carrier liquid during milling, when the volume of simulant waste required increases the use of isopropanol is no longer possible, as using large volumes of solvent is hazardous. Therefore, NNL utilised water as a carrier liquid, which introduces additional drying and bake out requirements to prevent arising issues during HIPping, as discussed above. Further work would be required to ascertain if scale up is possible, and would need to investigate alternative routes for producing the simulant wetox waste.

4 Organic Solids and Ion Exchange Resins

4.1 IRIS Process (CEA)

4.1.1 Description of the IRIS process

The ashes considered in these studies come from the IRIS incineration pilot process (Installation for Research on Incineration of Solids) developed at CEA Marcoule for R&D support and devoted to the treatment of the organic waste contaminated by α-emitting actinides from glove boxes in the nuclear industry. This pilot is working exclusively under inactive environment, and the ashes produced come from the incineration of a mix of different organic solids and IER resins (Figure 4-1). This leads to a volume reduction of the waste by about a factor of 30. IRIS is a three-step process implemented in rotating kilns. The first step consists in oxidative pyrolysis at 550 °C, producing pitch that is then calcined at 900 °C in oxygen-enriched atmosphere. The off-gases arising from the thermal treatments include a volatile hydrocarbon fraction that is oxidized at 1100 °C in an afterburner. This multistep process has two advantages. The elimination of chlorine at low temperature in the pyrolyser limits corrosion problems and allows operation with low gas flow, which also limits particle entrainment. Adding oxygen during the pyrolysis step oxidizes the heavy hydrocarbons that produce tars capable of forming deposits in the ducts. Forming during the pyrolysis step, the pitch drops into the calciner which is a rotary kiln heated at 900 °C. The pitch remains around 2 hours in this furnace and is transformed into ashes having a very low carbon content (< 1%). Before discharge to atmosphere, the gas stream is submitted to caustic scrubbing to eliminate the volatile acids. The material balance in the process is about as follows: a feeding rate of 4 kg h^{-1} produces around 1550 g h^{-1} of pitch, 111 g h^{-1} of ashes and 47 g h^{-1} of dust.

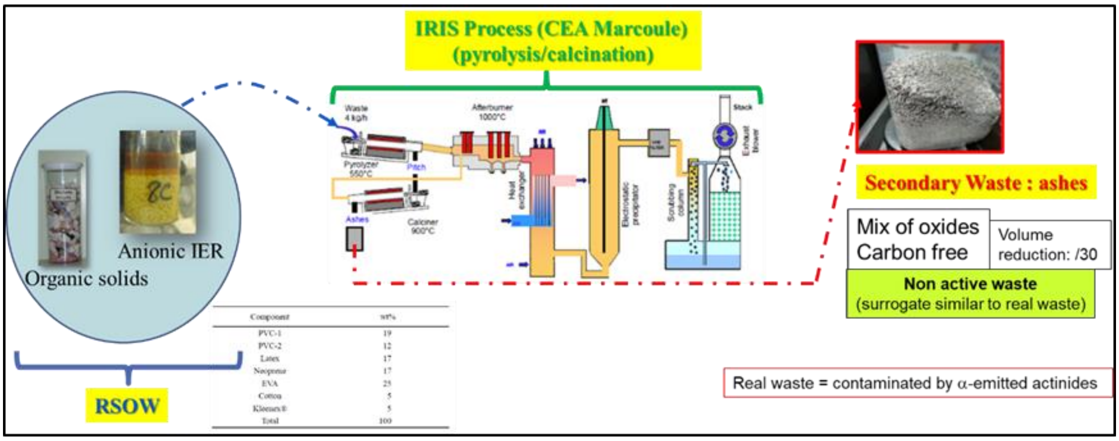

Component	wt%
PVC-1	19
PVC-2	12
Latex	17
Neoprene	17
EVA	25
Cotton	5
Kleenex®	5
Total	100

Figure 4-1. Description of the IRIS process.

4.1.2 Chemical and structural characterization of the ashes

The ashes produced have a high flying behaviour with a density of 0.2 g cm^{-3} and their particle size is mainly centered between 0.1 to 1 mm (Figure 4-2).

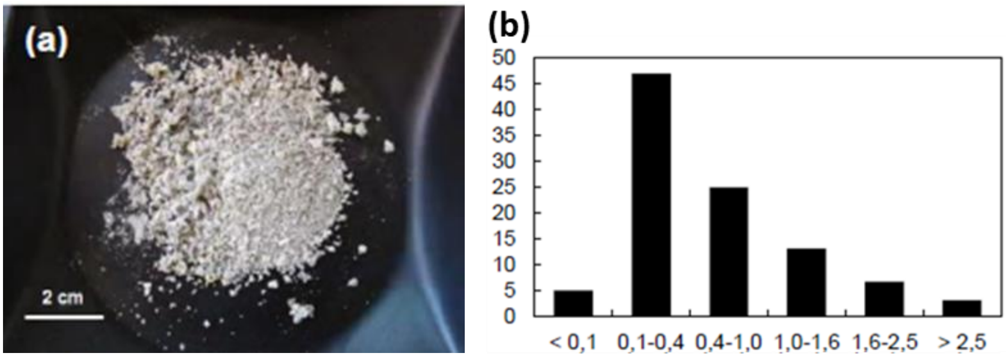

Figure 4-2. Photo showing IRIS ashes general morphology) and IRIS ashes granulometric class.

Chemical analysis shows that ~75 wt. % of the material consists of SiO_2 + Al_2O_3 + CaO, with further contributions from P_2O_5, K_2O, ZnO, MgO (see Table 4.1). A number of minor components are also present.

Table 4-1. Chemical analysis of the IRIS ashes.

Component	**Weight %**
SiO_2	29.35
Al_2O_3	28.46
CaO	13.55
P_2O_5	4.19
K_2O	3.61
ZnO	7.17
MgO	4.53
Cl	1.74
SO_3	1.41
Na_2O	0.95
TiO_2	0.69
Fe_2O_3	0.63
NiO	0.61
Bi_2O_3	0.13
BaO	0.15
Cr_2O_3	0.08

SEM and structural characterizations indicates that the micro particles are very porous and are partially amorphous. The crystalline phases present are ringwoodite and anorthite.

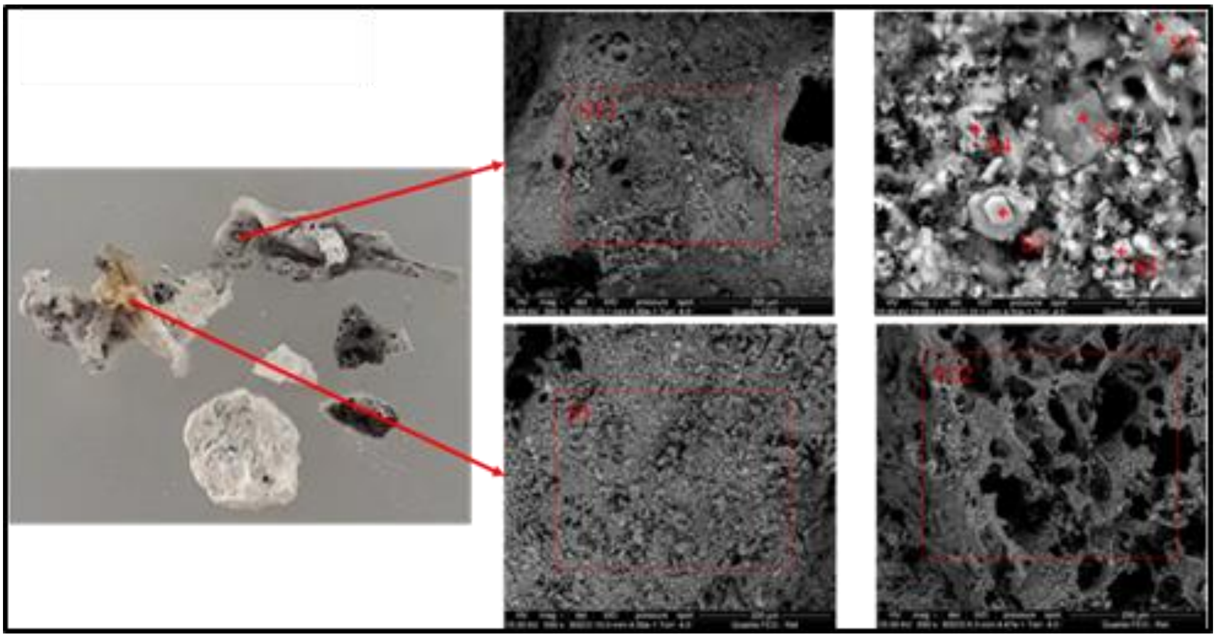

Figure 4-3. SEM analysis of the IRIS ashes.

4.2 Compaction IRIS Ashes (CEA)

The immobilization of the ashes waste using different routes was studied, with the objective being to obtain a densified monolith.

The first route is compaction. Ashes are shaped to get pellets obtained either starting from the raw ashes, either from a mix of ashes and glass as vitrification agent. The pellets were then heat-treated to get a densified and sintered monolith. The use of an adjuvant made of sodium silicate as part of this process was evaluated.

The shaping route with the addition of glass was not continued further, because in the proportions tested (30% borosilicate glass), the material shaped by pressing proved to be very porous and extremely fractured. We therefore only continued the shaping route of ash alone with a binder addition (sodium silicate in a content of about 5%).

Pellets of 10 mm in diameter and weighing 0.5 g were uniaxially pressed using pressures ranging from 64 to 200 MPa. The best mechanical performance was achieved with the pellets pressed using 200 MPa (see Figure 4-4).

Granulates were prepared using a granulator mixer and the effects of operating speed, granulation times and water addition have been evaluated. The best parameters to obtain quite a homogeneous granulate size have been determined; however, the granulates have low mechanical strength, making them very difficult to handle, and their overall mechanical performance are difficult to assess. The optimal conditions obtained are not given in this report because they constitute data that the CEA wishes to protect.

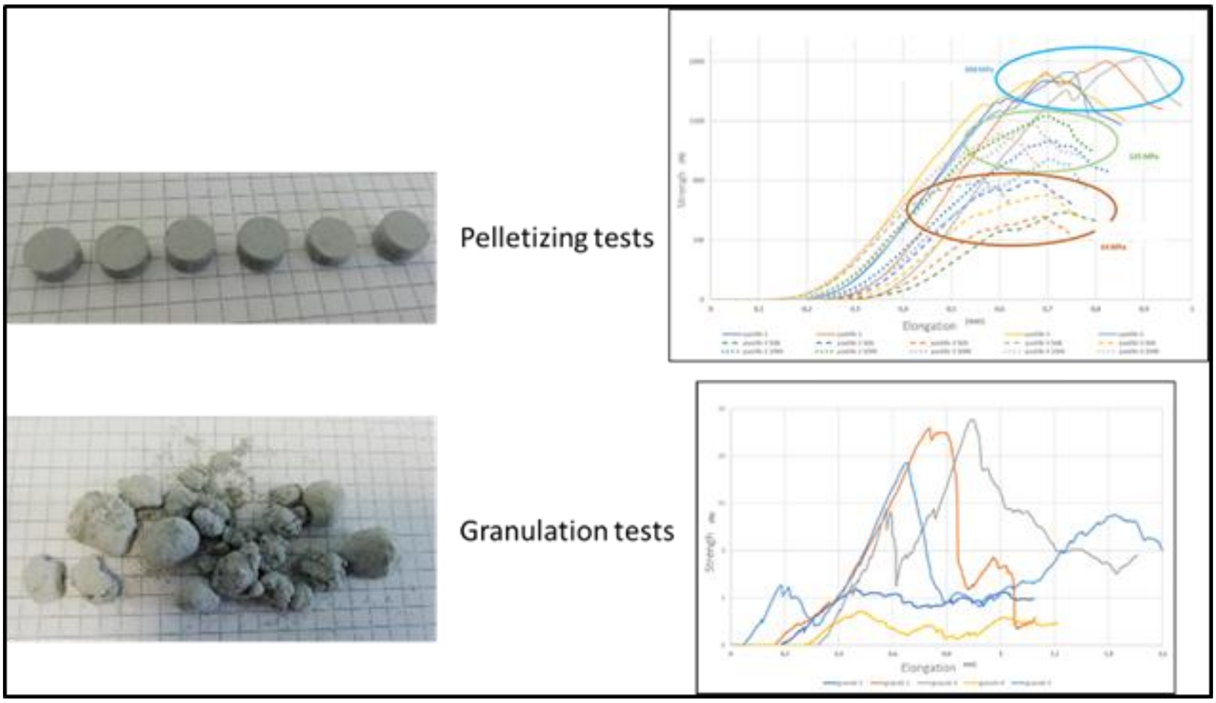

Figure 4-4. Mechanical characterizations of the pellets and granulates.

In a second step, these different shaped ashes were heat treated in a classical lab furnace at 1100 °C for during 3 h. For both shapes, a densified material has been achieved, with a significant densification factor, especially for the pellet (see Figure 4-5).

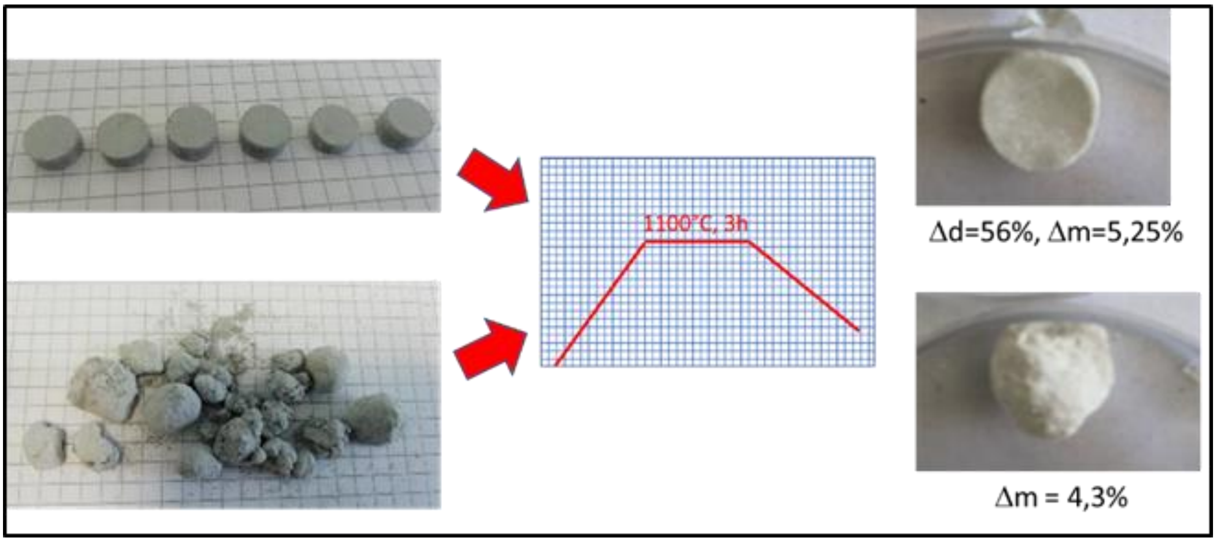

Figure 4-5. Thermal treatment of the pellets and granulates.

SEM analyses were carried out to check the microstructure of the pellets and granules after the heat treatment stage (Figure 4-6).

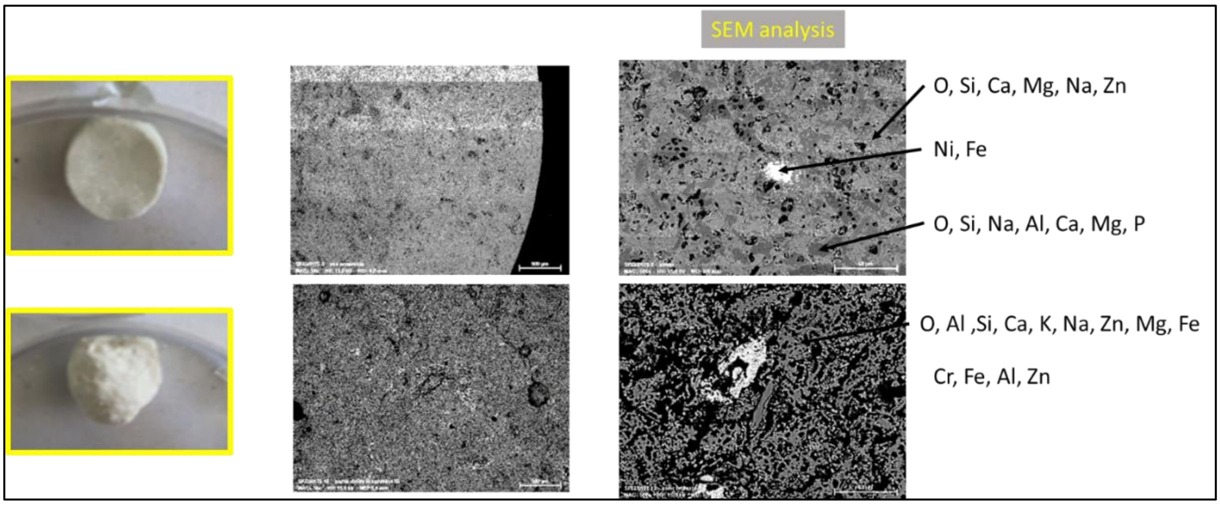

Figure 4-6. SEM analysis of the pellets and granulates

The microstructure of the pellet shows that the material has been correctly densified, with little porosity and a homogeneous distribution of the different phases where the different chemical elements of the starting ash can be found.

Logically, the granulate, even after heat treatment, appears much less densified than the pellet. This is consistent with the greater mechanical fragility observed in the raw pellet. However, from a microstructural point of view, the phases are also evenly distributed.

So the choice of one or other of the shaping methods (pellet or granulate) will be guided by the criteria of ease of shaping, taking into account the parameters of simplicity of the process, cost and minimisation of the production of scrap or secondary waste.

4.3 HIPping IRIS ASH (USFD)

Simulant IRIS ash was supplied to USFD by CEA (for chemical analysis see Table 4-1). The material has a loose, light grey appearance, with significant particle heterogeneity (see Figure 4-7). The ash weighed 305 g, and occupied a cylindrical space approximately 9 cm high by 12.5 cm wide (1104 cm^3), resulting in a bulk density of 0.28 g/cm^3.

Figure 4-7. Photograph of as-received simulant IRIS ash; the inner diameter of the comtainer is 12.5 cm.

Powder X-ray diffraction (XRD) analysis of the received ash is shown in Figure 4-8. This reveals a complex, diffraction pattern with both crystalline and poorly-crystalline components identified. Phase matching determined the presence of crystalline anorthite ($CaAl_2Si_2O_8$), diopside ($MgCaSi_2O_6$), chlorapatite ($Ca_5(PO_4)_3Cl$), and anhydrite ($CaSO_4$), in addition to a minor contribution from gypsum ($CaSO_4{\cdot}2H_2O$), and an unidentified poorly crystalline material at ~35 - 38° 2θ.

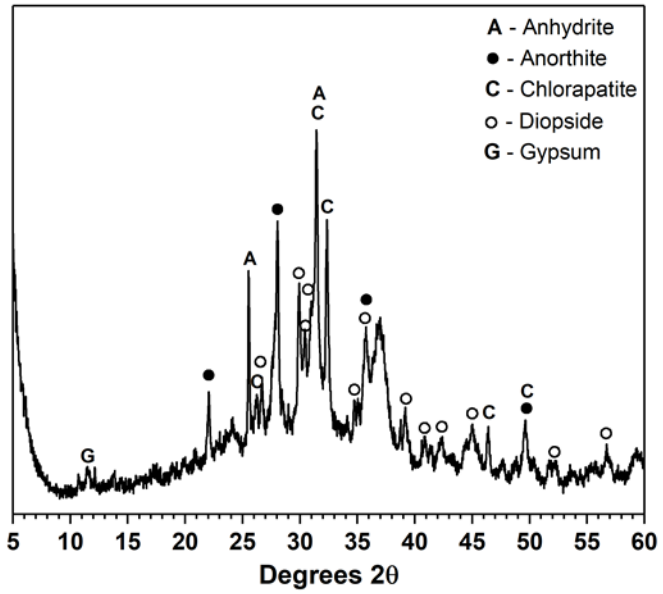

Figure 4-8. XRD pattern of as-received ash.

To process this material *via* HIP, it was decided to trial direct HIP of the as-received material. In parallel, several trials used varying additive materials. The additions were guided by the fact that although these ashes contain a significant proportion of glass forming elements, their relatively low SiO_2 content (29 wt. %), high Al_2O_3 content (28 wt.%) and only moderate alkali content (NaO + K_2O = ~8 wt. %), would impact likely glass formation under the available HIP conditions. As noted in Section 2.1 the HIP at USFD is limited to a continuous maximum temperature of 1320-1350 °C due to a) the melting point of the stainless steel canisters and b) the operation limit of the furnace.

A further potential variable is the particle size of the ash material. A smaller particle size may increase reactivity and produce a denser product, albeit at the cost of increasing the processing required. To determine the effect of both this, and the addition of fluxes, the following HIP trials were undertaken:

- HIP of as-received ash (no grinding, or additives)
- HIP of ground ash
- HIP of ground ash with 5 wt.% addition of sodium tetraborate
- HIP of ground ash with 5 wt.% addition of sodium aluminate

The processing conditions for all IRIS ash HIP canisters were: 1250 °C maximum temperature, 100 MPa pressure, 2 h dwell at maximum temperature, 10 °C/min ramp up. Each canister was baked out at 300 °C for at least 12 h to remove any residual water from the material before sealing the canister.

4.3.1 As-received ash

Direct HIP conditioning of the as-received ash was performed. 15.89 g of the as-received ash was packed into the canister. The canister was successfully welded, baked out and vacuum achieved (e.g. hermetically sealed). HIPping was successful, with a photograph of the final product (after sectioning off the bottom) shown in Figure 4-9. A solid product was formed, appearing to be heterogeneous in nature, based on different shades of grey detectable by eye, traversing the sample diameter.

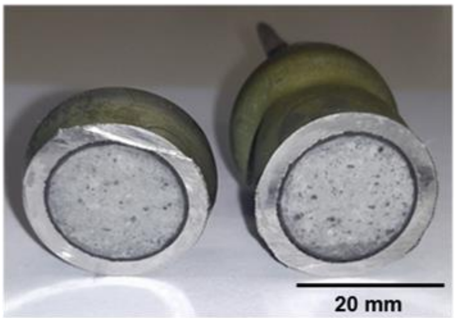

Figure 4-9. Photograph of sectioned canister after HIPping as-received ash.

XRD of the bulk material (Figure 4-10) revealed a highly crystalline product, with retention of many of the minerals present in the ash before HIPping, alongside the formation of some new mineral phases. Phase matching identified anorthite ($CaAl_2Si_2O_8$), diopside ($MgCaSi_2O_6$), chlorapatite ($Ca_5(PO_4)_3Cl$), leucite ($KAlSi_2O_6$), and spinel (‘$MgAl_2O_4$’, but likely with Zn, Fe and Cr substitutions). Anhydrite and gypsum have disappeared, whilst leucite and spinel have been formed. Some change in the crystalline assemblages may have occurred during the bake-out temperature, however typically (without sintering aids or milling) spinel and leucite tend to form in higher temperature environments >800-1000 °C [1-3].

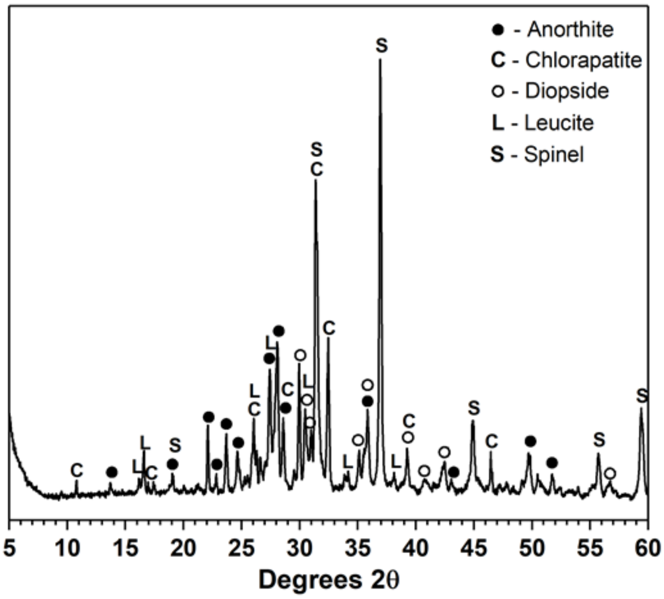

Figure 4-10. XRD pattern of HIPped as-received ash.

SEM analysis of the bulk material (Figure 4-11) revealed a heterogeneous product, which was partially vitrified. There is clear phase separation (evident more clearly by the elemental maps, e.g. Al, Si and Ca) and noticeable porosity. There appear to be several Zn-S hotspots, along regions rich in Ca-P-Cl regions, which were assigned to chlorapatite, as identified *via* XRD.

The interface between the bulk solidified ash and the canister wall (Figure 4-12) shows clear migration of Cr from the stainless steel canister into the bulk wasteform, with S migration into the steel. During processing, the ash appears to have formed a slightly aggressive melt (or partial melt), demonstrated by erosion of the internal canister wall (highlighted with arrows in Figure 4-13). The bulk material appears to have shrunk during cooling, resulting in a gap between the canister and the bulk material. Significant interaction with the canister wall is undesirable as this may damage the canister integrity (in a very aggressive melt held at high temperatures for longer during processing), and can result in an inhomogeneous wasteform due to introduction of steel elements (particularly Fe, Cr, Ni) which may form unexpected crystalline phases.

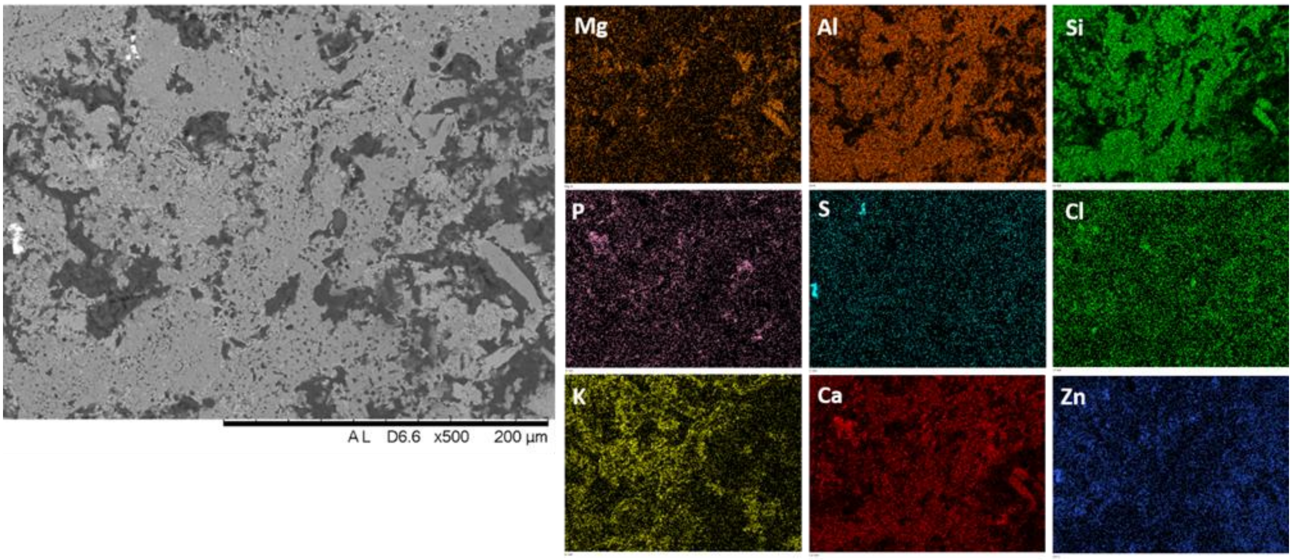

Figure 4-11. SEM micrograph and EDX maps of HIPped as-received ash.

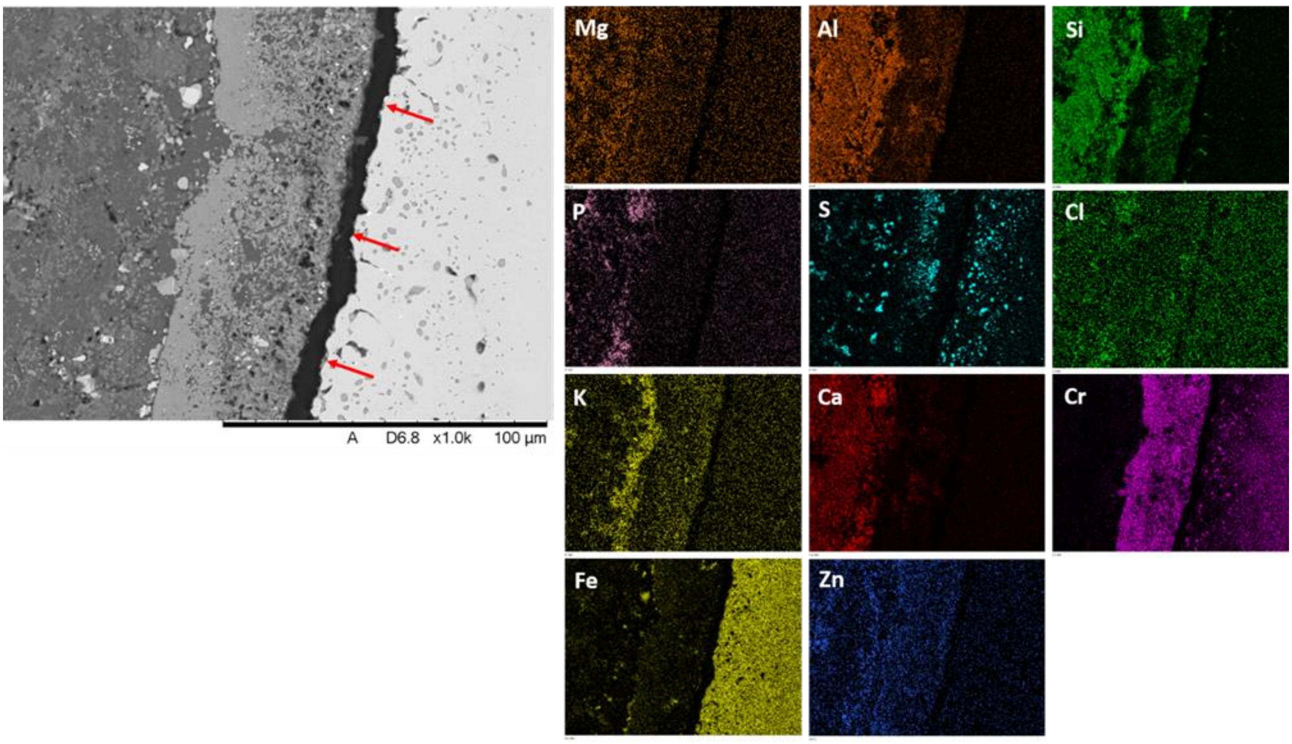

Figure 4-12. SEM micrograph and EDX maps of HIPped as-received ash / canister interface.

In summary, direct HIPing of the as-received ashes formed a solidified product which, at least partially, melted to form a crystalline multi-phase wasteform. Significant porosity was observed, giving rise to a lower density product overall. Such porosity may influence the aqueous durability of the wasteform through introduction of high surface area. The as-received ash deleteriously interacted with the internal stainless steel canister wall, although not enough to risk the structural integrity of the canister.

Further optimisation of this wasteform was undertaken *via* size reduction of the ash, with a view to enhancing the solid-state reaction and minimising porosity, and also through addition of chemical fluxes to lower the melting point.

4.3.2 Size reduced ash (ground, no additives)

This HIP trial tested the effect of size reduction *via* grinding on the final wasteform properties. The IRIS ash is extremely friable; therefore, manual hand grinding (using a pestle and mortar) was utilised rather than ball milling.

To prepare the canister, 20 g of as-received ash was hand ground for 5 minutes in a porcelain pestle and mortar. 19.35 g of powdered material was packed into the canister (using the aforementioned method), which was then processed as per the standard for these IRIS ashes: HIP canister bake-out and evacuation and subsequent HIPing (1250 °C, 100 MPa for 2 h).

The HIP processing was successful. After removal of the canister top, bottom, and side walls, a monolith was obtained, photographed in Figure 4-13. This was a solid product, with clear discoloration where the wasteform was touching the internal canister walls.

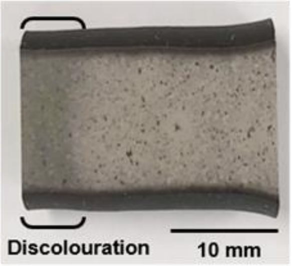

Figure 4-13. Photograph of HIPed ground ash, after removal from canister.

XRD analysis of the bulk material (Figure 4-14) exhibited the same crystalline assemblage as the HIPped as-received (unground) ash sample, with anorthite ($CaAl_2Si_2O_8$), diopside ($MgCaSi_2O_6$), chlorapatite ($Ca_5(PO_4)_3Cl$), leucite ($KAlSi_2O_6$), and spinel (‘$MgAl_2O_4$’, but likely with Zn, Fe and Cr substitutions). This wasteform was extremely crystalline, with many overlapping reflections. In comparison with the as-received HIPped sample (Figure 4-11), the intensity of the XRD reflections was increased, suggesting that the size reduction process resulted in increased crystallinity upon HIP processing.

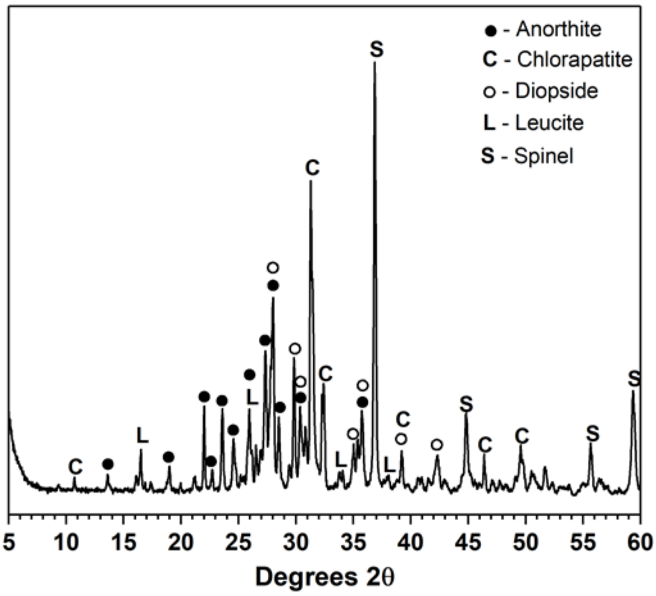

Figure 4-14. XRD pattern of HIPped ground ash.

SEM of the bulk material (Figure 4-15) revealed a heterogeneous material, with a much reduced porosity compared to the HIPped unground ash. There is a clear phase separation, with Mg and Zn anti-correlated with Si. This suggests that Zn may be incorporated within the Mg/Zn-bearing spinel phase identified by XRD. The original wasteform-canister interface (Figure 4-16) has interacted with the ash during processing, with pieces of steel embedded within the wasteform up to 100 µm away from the canister wall (spots a & b in Figure 4-16). As for the unground HIP sample, there was a clear alteration region at the canister-sample interface.

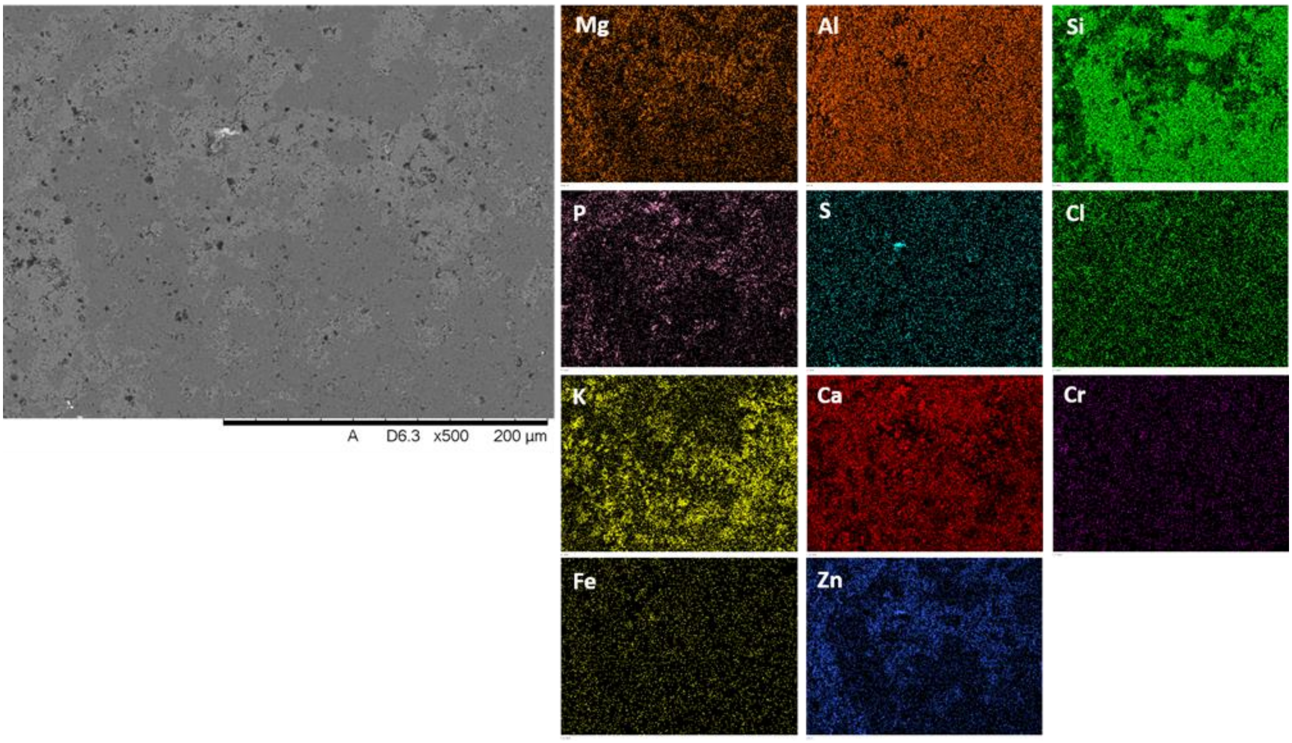

Figure 4-15. SEM micrograph and EDX maps of HIPped ground ash.

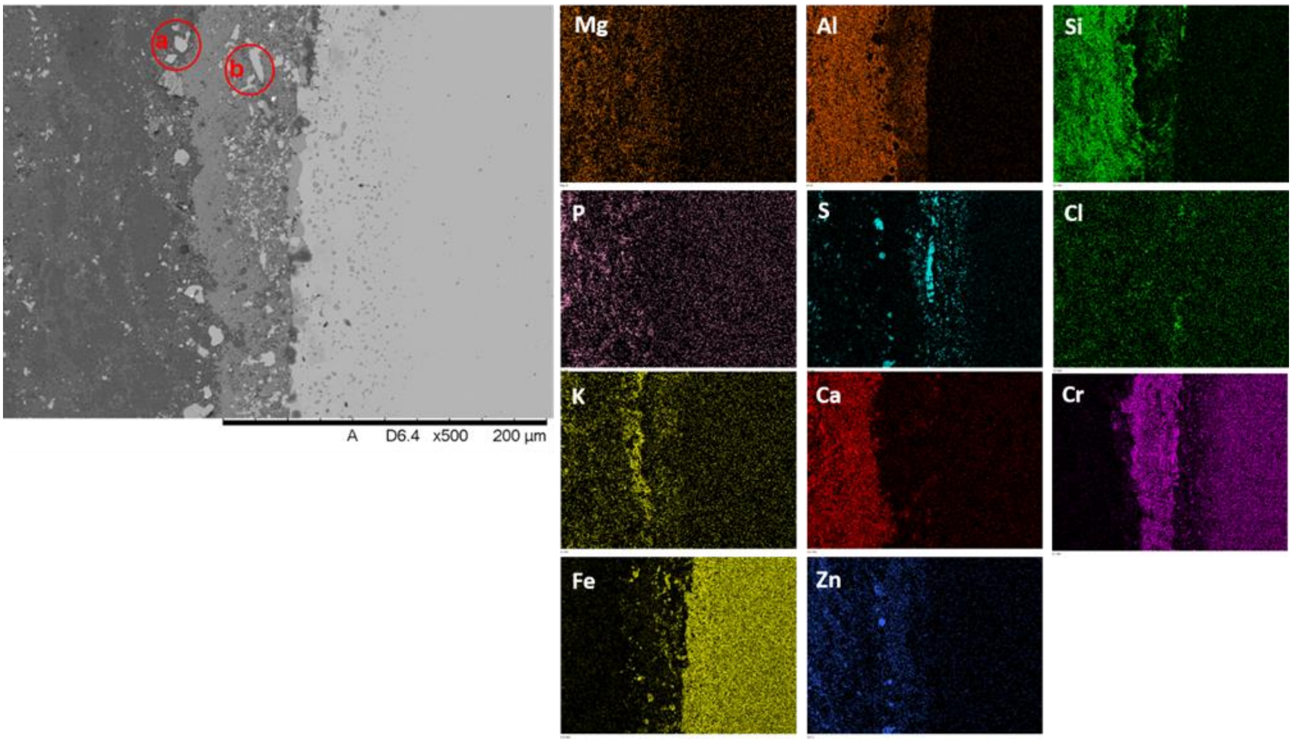

Figure 4-16. SEM micrograph of HIPped ground ash / canister interface.

In summary, gentle dry grinding of the IRIS ash produced a solidified and dense wasteform. There was a clear phase separation in the final product, however with extensive high temperature solid-state reactions (potentially due to the increased surface area from grinding). The sample was easily removed from the HIP canister without any cracking of the solid monolith. As such, this formulation appeared to be more successful than the unground HIP trial (primarily due to greater reaction and less obvious widespread porosity) and was taken forward for dissolution testing under WP 6.6.

4.3.3 Size reduced ash with sodium aluminate (ground, 5 wt% $NaAlO_2$)

In an attempt to lower the temperature of reaction, and to promote glass formation, an alkali additive was included in the formulation. Sodium aluminate ($NaAlO_2$) powder, often utilised in glass-forming applications, was mixed with the as-received ash, as follows: 19 g of as-received ash was mixed with 1 g of sodium aluminate (technical grade, Fisher Scientific) to create the 5 wt. % addition of $NaAlO_2$. The combined powder was hand ground for 5 minutes in a porcelain pestle and mortar to homogenise (in accordance with the previous trial). 19.18 g of the combined, ground material was used to pack the HIP canister using the standard method discussed previously.

HIP processing (1250 °C and 100 MPa for 2 h) was successful, leading to the formation of a dense solidified monolith. A photograph of the resulting product after canister removal is shown in Figure 4-17.

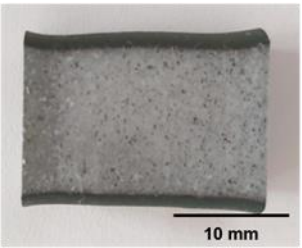

Figure 4-17. Photograph of HIPped ground ash with sodium aluminate, after removal from canister.

XRD analysis of the bulk material again revealed similar crystalline phases, with anorthite ($CaAl_2Si_2O_8$), diopside ($MgCaSi_2O_6$), chlorapatite ($Ca_5(PO_4)_3Cl$), leucite ($KAlSi_2O_6$), and spinel ('$MgAl_2O_4$', but likely with Zn, Fe and Cr substitutions). The material is very crystalline, with particularly intense reflections for spinel and chlorapatite when compared to the previous trials (see Figure 4-18).

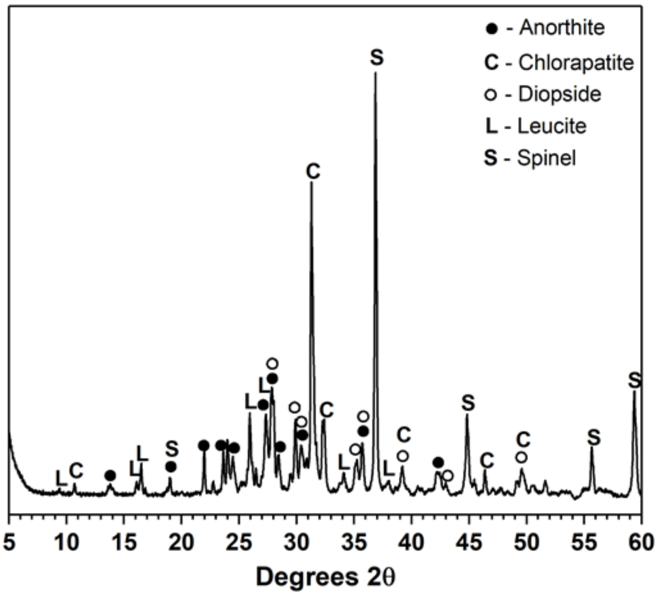

Figure 4-18. XRD pattern of HIPed ground ash with sodium aluminate.

SEM of the bulk material (Figure 4-19) revealed a much more homogeneous product than for samples without additives. There remains some porosity, although this was spherical in nature indicating that it formed within a melt. There was evidence of some phase separation, especially evidenced by the K EDX map (Figure 4-19-K). Very small crystallites < 5 µm were present throughout the sample, with larger clusters clearly enriched in P (likely chlorapatite based on XRD analysis). The canister wall (Figure 4-20) appears to have been interacted with the wasteform with some Cr diffusing from the steel, forming a particularly strong band enriched in Cr. There was migration of S (from the IRIS ash) into the steel canister, and a formation of Zn-S enriched particles near the canister wall (compared to no visible hotspots in the bulk material in Figure 4-20). These are likely zinc sulphide, formed under the reducing conditions imposed by the stainless steel canister. Although erosion of the canister wall occurred, it appeared to be less aggressive than for the as-received ash (both packed unground, and the ground sample).

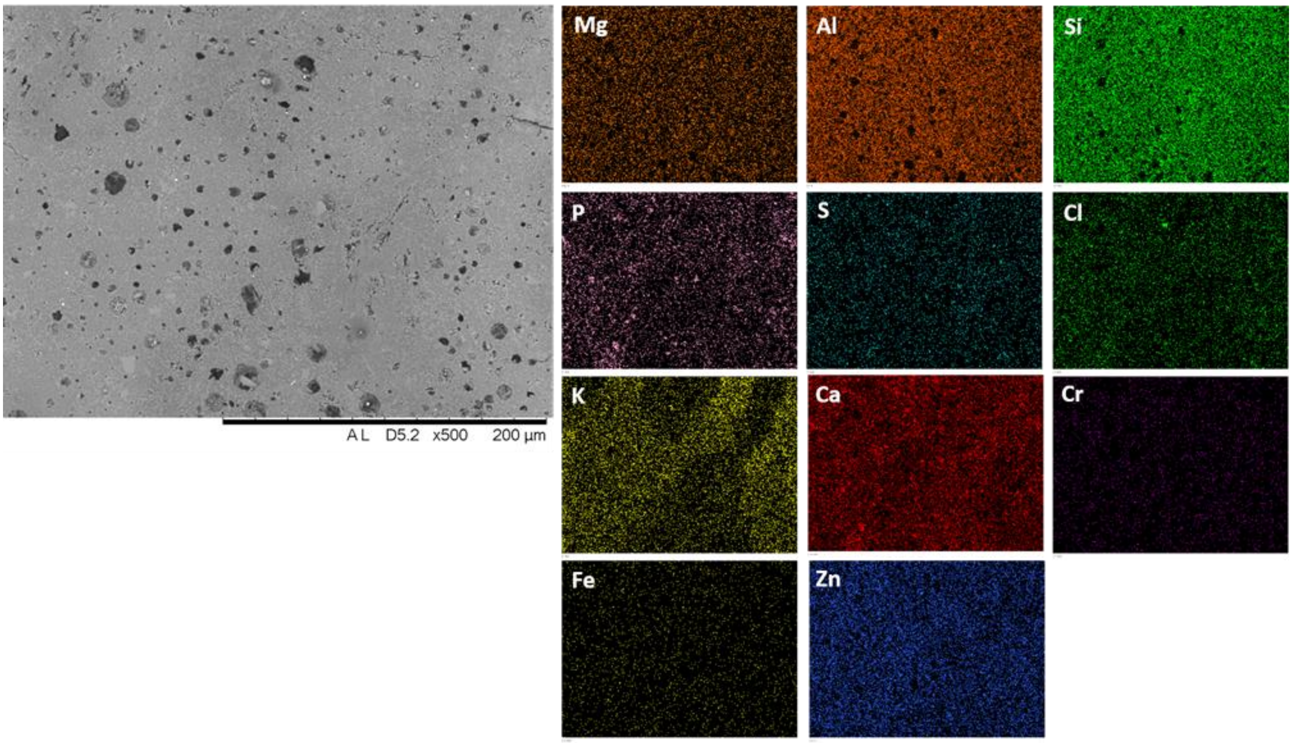

Figure 4-19. SEM micrograph and EDX maps of HIPped ground ash + sodium aluminate.

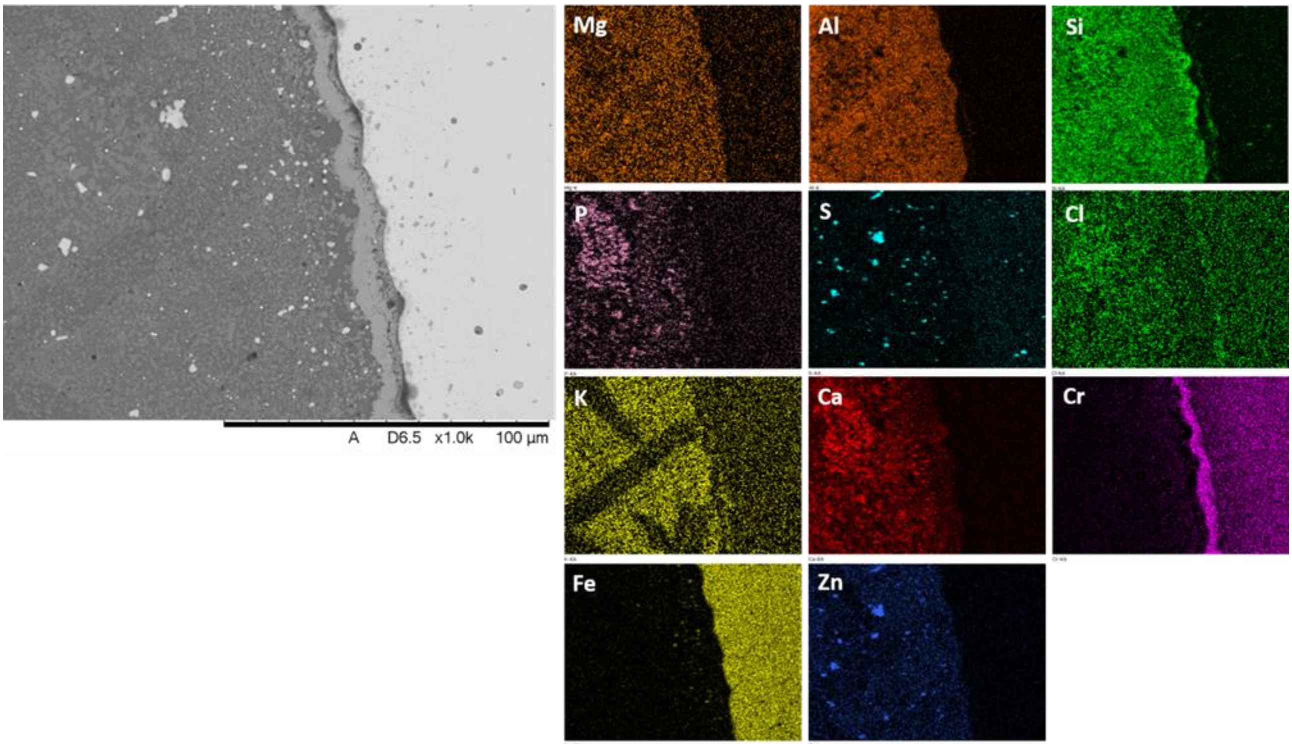

Figure 4-20. SEM micrograph of HIPped ground ash + sodium aluminae / canister interface.

In summary, the addition of 5 wt. % sodium aluminate into the IRIS ashes appears to have successfully formed a solidified wasteform. The final product was a dense material, which did not break or shatter on removal from the HIP canister. Although still a largely crystalline material, the presence of spherical pores indicated that some ash melting and consolidation occurred. Due to the success of this formulation, this wasteform was taken forward for dissolution testing under WP 6.6.

4.3.4 Size reduced ash with sodium tetraborate (ground, 5 wt% $Na_2B_4O_7$)

In a further attempt to form a more homogeneous product, the addition of sodium tetraborate ($Na_2B_4O_7$) was trialled. This is a more traditional flux in glass making, and acts effectively to reduce the melt temperature. The material was processed in the same way as for the previous addition. 19 g of as-received ash was mixed with 1 g anhydrous sodium tetraborate (99%, Sigma-Aldrich). The combined material was hand ground for 5 minutes in a porcelain pestle and mortar to homogenise the batch. The blended, ground material was packed into the HIP canister to a total of 19.26 g.

The HIP process (1250 °C and 100 MPa for 2 hours) was successful, with a photograph in Figure 4-21 depicting the solid monolith following canister removal, with the IRIS ash densified into a solid product.

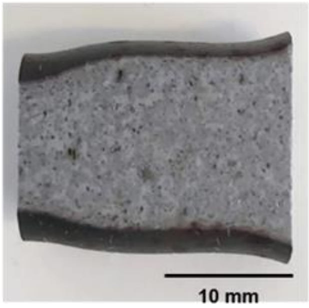

Figure 4-21. Photograph of HIPped ground ash + sodium tetraborate, after removal from canister.

XRD analysis was undertaken on monoliths (from cutting the material out of the canister) both the bulk material, and on the interfacial zone (the black section at the top and bottom of Figure 4-19). The interfacial region (Figure 4-20, defined here as the ‘outside face’ of the HIPed ground ash with sodium tetraborate) revealed a poorly crystalline diffuse reflection characteristic of the formation of a glassy material (i.e. with no long-range order). Also observed were diffraction peaks indexed as zincochromite ($ZnCr_2O_4$) / magnetite (Fe_3O_4), haematite (Fe_2O_3), which are challenging to distinguish since they occupy the same crystal structure.

XRD analysis of the bulk material (Figure 4-22) revealed a very different phase assemblage when compared with the other HIPped wasteforms investigated in this study. Only spinel ($ZnAl_2O_4$ / $MgAl_2O_4$ likely) and chlorapatite ($Ca_5(PO_4)_3Cl$) reflections were visible, in addition to a region of diffuse scattering, indicating the formation of a glassy phase. There were no reflections for any crystalline silicates remaining from the original ash (e.g. anorthite, diopside, etc.), indicating that the extent of wasteform decomposition was the greatest of all the formulations trialled.

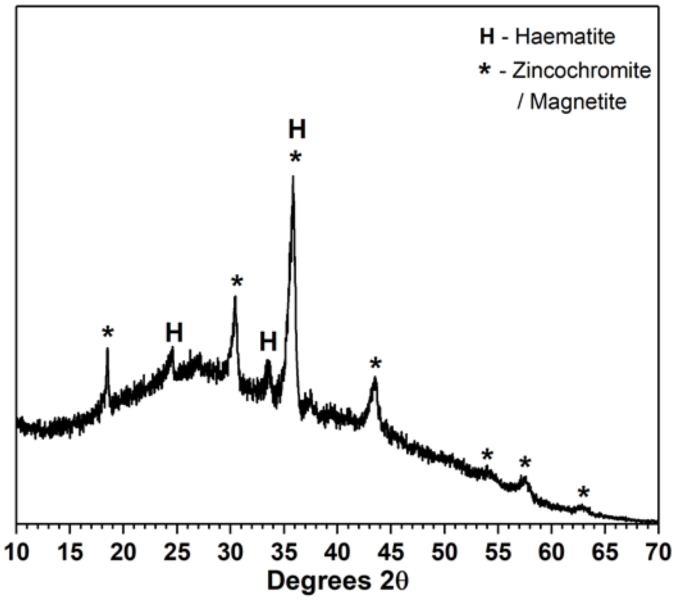

Figure 4-22. XRD pattern of the outside face of HIPped ground ash with sodium tetraborate (after canister removal).

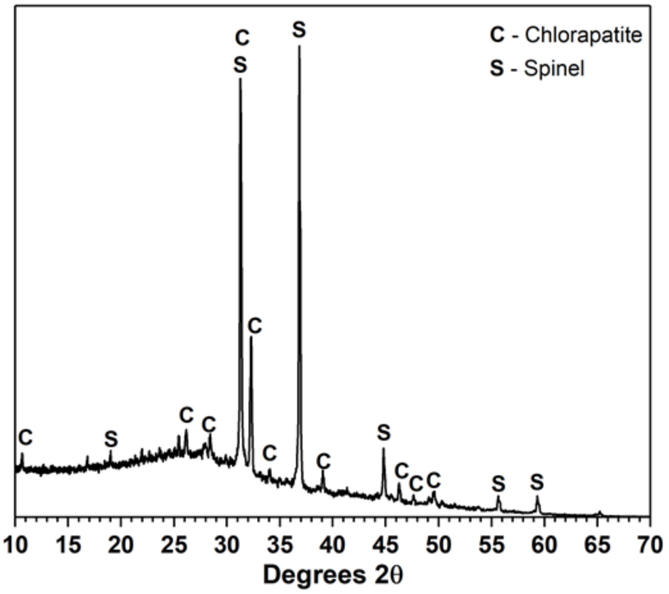

Figure 4-23. XRD pattern of the bulk material of HIPped ground ash with sodium tetraborate.

SEM analysis of the bulk material (Figure 4-24) shows a morphology indicative of crystalline materials incorporated within a glassy matrix. Larger crystallites from ~10-50 µm (including some elongated crystallites) were assigned as chlorapatite (elemental maps: Cl, Al, Si) and the much smaller crystallites as spinel. The canister-ash interface (Figure 4-25) shows Cr migration into the melt (in agreement with previous samples); however, this reaction appeared to be less corrosive than previous formulations (as received, ground, and with sodium aluminate), as evidenced by the retention of the largely linear canister edge. The Cr migration resulted in the formation of zincochromite in a narrow band near the canister wall (spot a, Figure 4-25). As per previous samples, S hotspots are observed in the canister (highlighted in spot b, Figure 4-25).

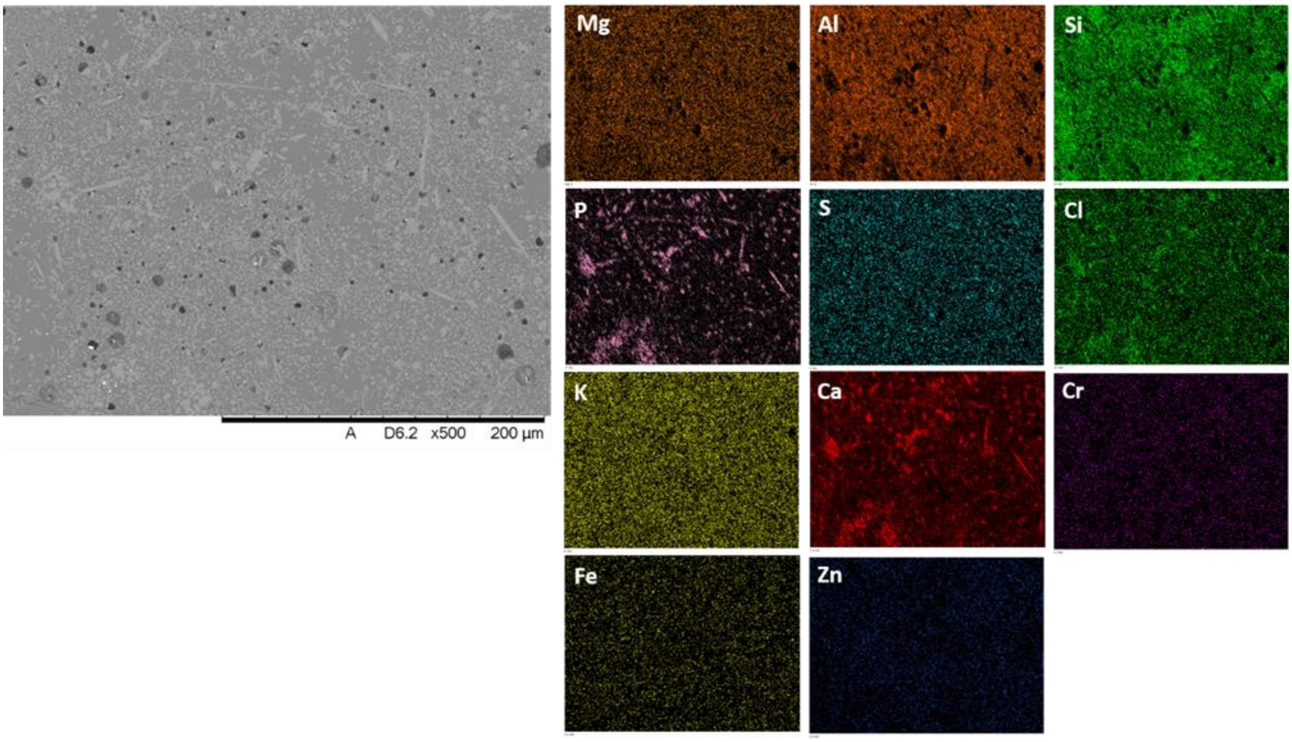

Figure 4-24. SEM micrograph and EDX maps of HIPped ground ash with sodium tetraborate.

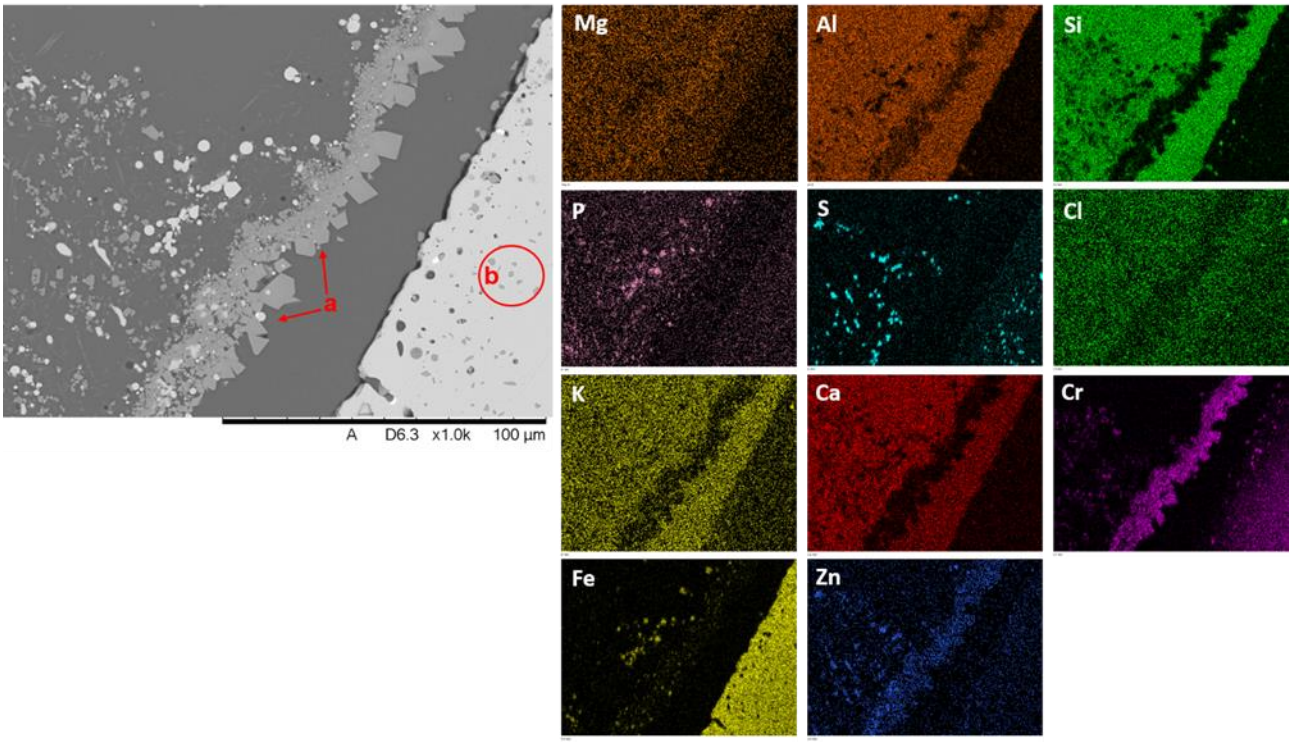

Figure 4-25. SEM micrograph and EDX maps of HIPped ground ash with sodium tetraborate / canister interface.

Sodium tetraborate was the most successful additive, resulting in a glass-ceramic material in which the ash was almost completely melted. Although some canister-wasteform interaction occurred, it appeared to be less aggressive towards the canister than other formulations. Due to these positive outcomes, this formulation was also taken forward for dissolution trials in WP 6.6.

5 Wood Ash (Chernobyl) (KIPT/USFD)

Due to the invasion of Ukraine by Russia, all progress towards KIPT task deliverables was halted in 2022.

KIPT were due to undertake lab scale tests on ash arising from incineration of non-radioactive wood ashes (as simulant material for contaminated wood), encapsulating this within a geopolymer cement. These ashes arise from the treatment of contaminated wood from around Chernobyl Nuclear Power Plant site, using an experimental incinerator built with financial support from the European Commission. The volume of contaminated material is greatly reduced via incineration, but the ash cannot be stored for a long time in this form and requires immobilisation.

- Furnace sintering
- Hot Pressing (HP)
- Hot Isostatic Pressing (HIP)

Materials were to be experimentally characterised and the stability tested using conventional laboratory techniques (XRD, DTA/TGA)

Prior to the Russian invasion good progress was made at KIPT towards the objectives under WP 6.5. Two avenues for investigation were undertaken: using a geopolymer-ash matrix, and formation of fluorapatite from ash.

5.1 Geopolymer + Ash matrix

A geopolymer matrix was product, using metakaolin, sand, H_2O, KOH, and K_2SiO_3. This resulted in a 70% geopolymer, 30% ash blend being mixed, and left to cure for up to 28 days. The hardened material was then crushed, cold pressed into a pellet, and taken forward for densification *via* sintering, HP, and HIP (Figure 5-1).

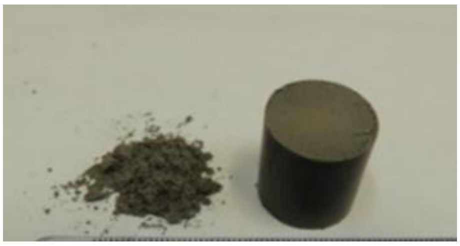

Figure 5-1. Crushed geopolymer-ash material (left), and pressed green body of the same material ready for thermal treatment (right).

A simulant ash was produced *via* pyrolytic processing of wood, due to the radioactive nature of the real ashes. The as-obtained particles were photographed and shown in Figure 5-2. Laboratory analysis of the simulant radioactive ash *via* XRD revealed a multi-phase material, including calcite ($CaCO_3$), quartz (SiO_2), hydroxyapatite ($Ca_5(PO_4)_3(OH)$), calcium oxyphosphate ($Ca_4(PO_4)$), and potassium chloride (KCl), as demonstrated in Figure 5-3.

Figure 5-2. Obtained simulant ash from wood pyrolysis.

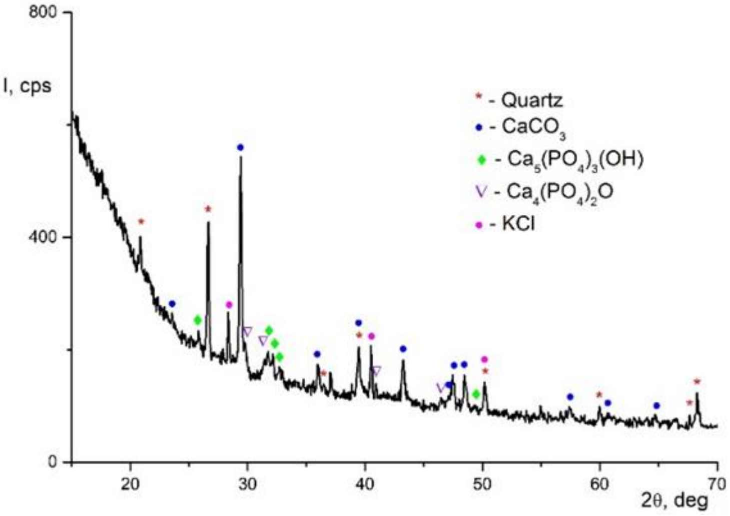

Figure 5-3. XRD diffraction pattern of the simulant ash.

The production of a monolithic geopolymer sample both with, and without, this ash was undertaken successfully. XRD analysis of the geopolymers are shown in Figure 5-4, with a 100% geopolymer, and a 70% geopolymer / 30% ash sample analysed. Crystalline phases within the former was determined to be only quartz (SiO_2), while the addition of ash to the geopolymer resulted in the formation of quartz, $CaCO_3$ and KCl. Neither of these materials demonstrated any cracking after 28 days of curing, and both formed solid materials.

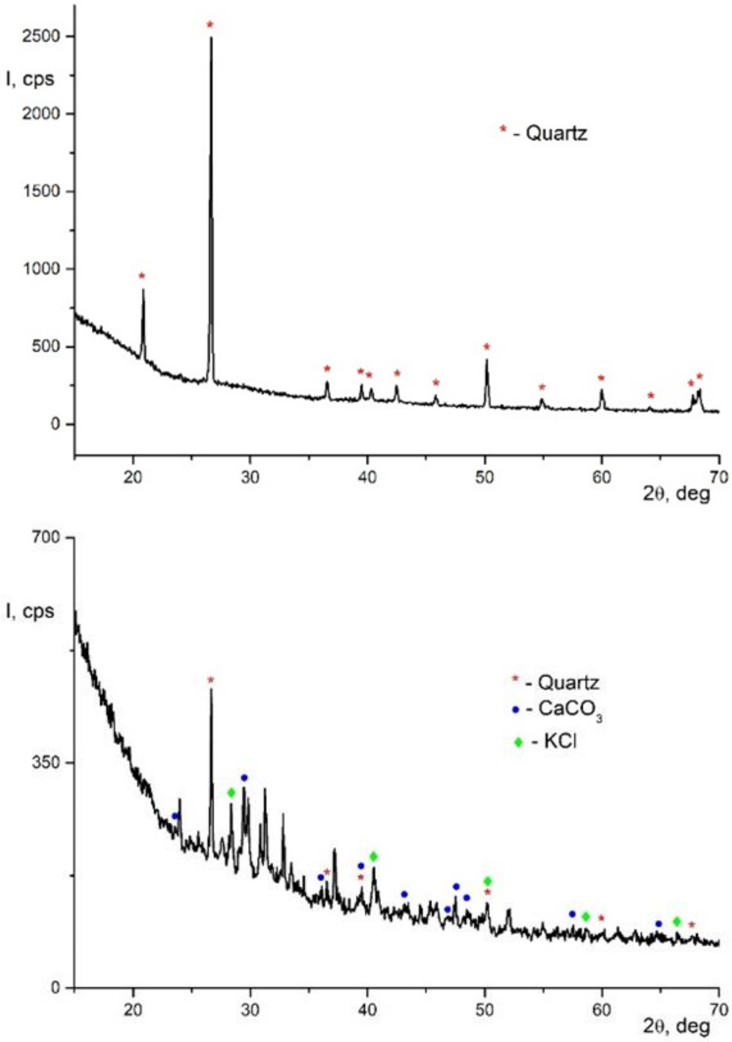

Figure 5-4. XRD reflections for 100% geopolymer (top), and 70% geopolymer – 30% ash (bottom).

5.1.1 Geopolymer + Ash matrix + Sintering trials

The 30% ash-containing sample was taken forward for thermal treatment, by sintering and hot pressing methods. Sintering was undertaken over a range of temperatures from 800-1050 °C, over a 3 h run, holding at the maximum temperature for 1 h. Figure 5-5 shows a pellet of the 30% ash sample after sintering at 1020 °C. Increasing the sintering temperature resulted in higher density (Table 5-1) up to 1020 °C, with a further increase to 1050 °C not leading to any further increase in density.

Figure 5-5. Pellet of 70% geopolymer, 30% ash after sintering at 1020 °C.

Table 5-1. Pellet density for 30% ash samples after sintering.

T, °C	Density, g/cm^3	%age theoretical density
800	1.89	70
900	2.10	78
1020	2.30	85
1050	2.30	85

Hot pressing the 30% ash sample was undertaken at 920 °C during a 60-minute run, with 30 minutes at the maximum temperature, utilising a pressure of 40 MPa. Pellets were wrapped in a copper foil to reduce any interaction with the graphite mould. The resulting density of the pellets after HP was 2.57 g/cm^3 (95% theoretical density). Figure 5-6 shows pellets after hot pressing, with XRD analysis of these pellets revealed the presence of quartz (SiO_2), calcium silicate ($CaSiO_3$), and leucite ($KAlSi_2O_6$), as per Figure 5-7.

Figure 5-6. Pellets of 70% geopolymer, 30% ash after hot pressing at 920 °C.

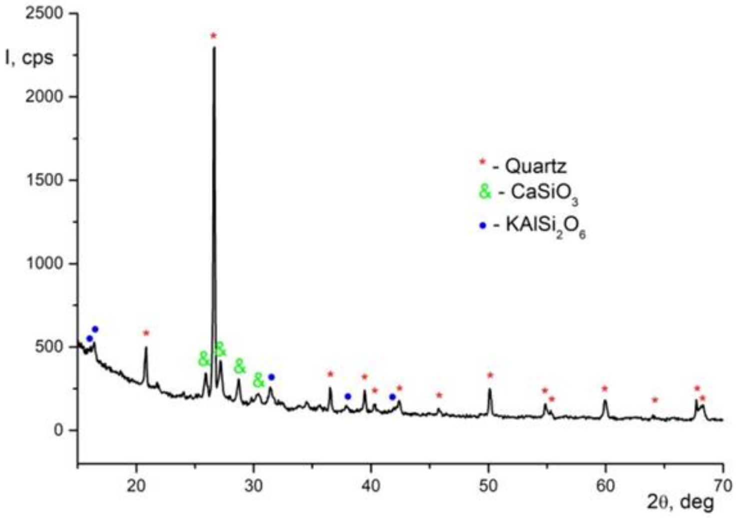

Figure 5-7. XRD pattern of the 70% geopolymer, 30% ash sample after hot pressing.

5.1.2 Geopolymer + Ash matrix + HIP

Pellets were then prepared for Hot Isostatic Pressing (HIP) *via* pressing 10 mm × 7 mm pellets (typical mass 1.0-1.1 g), of which multiple pellets were stacked within a cylindrical stainless steel HIP canister, depicted in Figure 5-8.

Figure 5-8. HIP canister prepared with pellets of 70% geopolymer, 30% ash.

5.2 Fluorapatite + Ash matrix

An alternative avenue for investigation was the formation of fluorapatite ($Ca_5(PO_4)_3F$) as a stable mineral phase for these ashes, instead of incorporation within a geopolymer matrix. The main phases within the ash include calcite, hydroxyapatite, and calcium oxyphosphate. The addition of some calcium orthophosphate ($Ca_3(PO_4)_2$) and calcium fluoride (CaF_2) in the right stoichiometric amounts, along with sintering at temperature, should drive the system towards the formation of fluorapatite.

The optimal amounts of additives for obtaining fluorapatite from the ash samples has been determined as:

- 50.8 wt.% ash
- 40.4 wt.% $Ca_3(PO_4)_2$
- 8.8 wt.% CaF_2

Thermal treatment of the powder mixture $Ca_3(PO_4)_2$ + CaF_2 + ash was undertaken at 1100 °C in air, for 3 h, with 0.5 h at the maximum temperature. XRD analysis of the resulting material after heating is shown in Figure 5-9, revealing the formation of $Ca_5(PO_4)_3F$ alongside $CaSiO_3$.

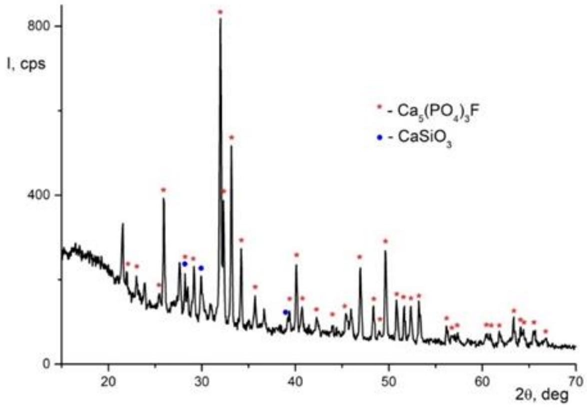

Figure 5-9. XRD pattern of the $Ca_3(PO_4)_2$ + CaF_2 + ash powder mixture after heat treatment.

Hot pressing of the powder containing fluorapatite was undertaken. Pellets were first prepared by cold pressing and sintering at:

- 1150 °C, 180-minute run (60 minutes at maximum temperature) = 2.56 g/cm^3 density (80%)

- 1200 °C, 180-minute run (60 minutes at maximum temperature) = 2.72 g/cm^3 density (85%)

5.2.1 Fluorapatite + Ash matrix + HP

Hot pressing to increase the density was performed at 1150-1200 °C, for a 1 h run (0.5 h at maximum temperature), with an applied pressure of 40 MPa. Unfortunately, hot pressing resulted in destruction of the samples (Figure 5-10). This is thought to be due to the graphite mold, from which carbon is able to enter the structure of the phosphates, resulting in sample instability and a decrease in thermal stability, with the consequential appearance of cracks and sample destruction. Due to this, it was decided to utilise HIP for future processing, as the pellets will be encapsulated by a stainless steel container, hopefully preventing sample destruction.

Figure 5-10. Pellet after hot pressing.

However, this work was not completed due to the impact of the Russian invasion.

6 Summary

This report has primarily focussed on the use of hot isostatic pressing, supported by some cold-press and sinter work, to immobilise four potential wastes: ion exchange resins; wet oxidation (wetox) wastes from Fenton oxidation; IRIS ashes and wood ashes.

HIPping of polymeric ion exchange resins was unsuccessful as the polymeric wastes started to break down during the process to weld on the can lid meaning that the HIP canisters could not be sealed.

In comparison small scale HIPping of the simulant wetox wastes was successful. The former produced a series of solid multi-phase ceramic wasteforms, in which the phase assemblage of the wasteforms can be driven towards spinel by the increasing the fraction of Fe_2O_3 in the batch. Some optimisation of the HIPping conditions may enable the production of a single phase spinel. Although some interaction between the HIP canister and the bulk material, to the detriment of the HIP canister wall was seen this was sufficient to warrant concern. Thus far larger scale HIPing of simulant wetox wastes to demonstrate the potential for scale up has not yet been successful.

Attempts to cold press pellets of IRIS ashes with additions of 30% borosilicate glass were unsuccessful and produced fractured samples. Treatment of the IRIS ashes by adding 5 wt. % sodium silicate and then either cold pressing or forming a granulate before thermal treatment produced successfully densified materials. After thermal treatment the pressed pellet samples were found to be more dense than the granulate.

HIPping of the as-received IRIS ashes formed a solidified product which, at least partially, melted to form a crystalline multi-phase wasteform. Gentle dry grinding of the IRIS ash produced a solidified and dense mutli-phase wasteform. The addition of 5 wt. % sodium aluminate into the IRIS ashes appears to have successfully formed a solidified wasteform. Sodium tetraborate was the most successful additive, resulting in a glass-ceramic material in which the ash was almost completely melted. Although some canister-wasteform interaction occurred, it appeared to be less aggressive towards the canister than other formulations. All of the latter three compositions were taken forward for durability testing under WP 6.6.

Initial work of wood ashes involved the use of geopolymers or fluorapatite coupled with cold pressing and sintering followed by hot pressing. Given the failure of the sample on hot pressing it was planned to HIP the samples to see if this would produce useful densified wasteforms. Further work on this part of the WP was prevented by the Russian invasion of Ukraine.

Overall HIPping of a wetox waste and an ash waste has been demonstrated at the small scale. As well as the microstructural characterisation of the wasteforms detailed here, the HIPped ash wasteforms have been taken forward for durability testing.

REFERENCES

[1] A.D. Mazzoni, M.A. Sainz, A. Caballero, E.F. Aglietti, Formation and sintering of spinels (MgAl2O4) in reducing atmospheres, Mater. Chem. Phys. 78(1) (2003) 30-37.

[2] S. Hashimoto, A. Yamaguchi, K. Fukuda, S. Zhang, Low-temperature synthesis of leucite crystals using kaolin, Mater. Res. Bull. 40(9) (2005) 1577-1583.

[3] N. Xie, J.L. Bell, W.M. Kriven, Fabrication of Structural Leucite Glass–Ceramics from Potassium-Based Geopolymer Precursors, J. Am. Ceram. Soc. 93(9) (2010) 2644-2649.

[4] D. Shishin, T. Hidayat, E. Jak, S.A. Decterov, Critical assessment and thermodynamic modeling of the Cu–Fe–O system, Calphad 41 (2013) 160-179.

[5] L.V. Díaz, J.O. Pacheco, M. Pacheco, F. Monroy, M. Emeterio, F. Ramos, Ion Exchange Resin and Clay Vitrification by Plasma Discharges, AIP Conference Proceedings 875(1) (2006) 184-187.

[6] İ. Kayacan, Ö.M. Doğan, Pyrolysis of Low and High Density Polyethylene. Part I: Non-isothermal Pyrolysis Kinetics, Energy Sources, Part A: Recovery, Utilization, and Environmental Effects 30(5) (2008) 385-391.

[7] I. Dubdub, M. Al-Yaari, Pyrolysis of Low Density Polyethylene: Kinetic Study Using TGA Data and ANN Prediction, Polymers 12(4) (2020) 891.